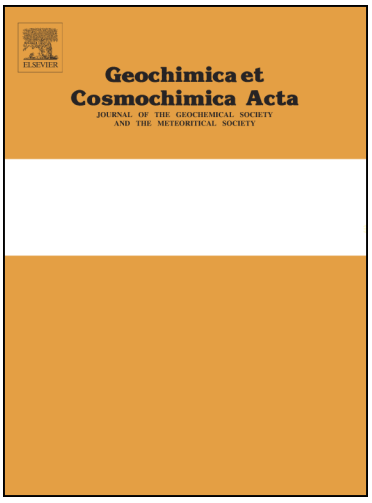

Assessing foraminifera biomineralisation models through trace element data of cultures under variable seawater chemistry

David Evans, Wolfgang Müller, Jonathan Erez

PII: S0016-7037(18)30138-8
DOI: https://doi.org/10.1016/j.gca.2018.02.048
Reference: GCA 10691

To appear in: *Geochimica et Cosmochimica Acta*

Accepted Date: 28 February 2018

Please cite this article as: Evans, D., Müller, W., Erez, J., Assessing foraminifera biomineralisation models through trace element data of cultures under variable seawater chemistry, *Geochimica et Cosmochimica Acta* (2018), doi: https://doi.org/10.1016/j.gca.2018.02.048

Assessing foraminifera biomineralisation models through trace element data of cultures under variable seawater chemistry

David Evans[a], Wolfgang Müller[b,c], Jonathan Erez[d]

[a]*School of Earth and Environmental Sciences, University of St Andrews, St Andrews, KY16 9AL, UK*
[b]*Department of Earth Sciences, Royal Holloway University of London, Egham, TW20 0EX, UK*
[c]*Institute of Geosciences, Goethe University, Frankfurt am Main, Germany*
[d]*Institute of Earth Sciences, The Hebrew University of Jerusalem, Jerusalem, Israel*

Abstract

The process by which foraminifera precipitate calcite from seawater has received much attention, in part because a mechanistic basis for empirical calibrations between shell chemistry and environmental parameters is desirable given their widespread application in palaeoceanography. The incorporation of fluorescent membrane-impermeable molecules into the shell demonstrates that seawater, transported by vacuolisation, is present at the site of calcification. However, recent discussion has focused on whether the calcium required for chamber formation is sourced predominantly by transmembrane Ca transport (TMT), with seawater vacuolisation playing a passive role, or vice versa. This debate has arisen in part because of the need to explain the low Mg/Ca ratio of most foraminifera compared to inorganic calcite. Here, we present trace element data of *Operculina ammonoides* and *Globigerinoides ruber*, a high-Mg shallow benthic, and low-Mg planktonic species respectively, cultured under variable seawater carbonate and elemental chemistries. We find that Mg incorporation in high and low-Mg species is characterised by an opposite response to the carbonate system, demonstrating

that the negative relationship between Mg/Ca and pH or [CO_3^{2-}] in several low-Mg foraminifera is not an intrinsic feature of foraminiferal (or inorganic) calcite precipitation. Therefore, any biomineralisation model must be able to explain why the mechanism by which seawater Mg/Ca is reduced is impacted by the carbonate system. Moreover, we show that trace element incorporation in *G. ruber* is consistent with Rayleigh fractionation from unmodified seawater except for Mg-removal, but in very poor agreement with a biomineralisation site [Ca] substantially elevated above that of seawater as required by the TMT hypothesis. In addition, any biomineralisation model must explain the nonlinear relationship between seawater and shell Mg/Ca, and the large number of seawater vacuoles observed in some species. Although there are important inter-species differences in biomineralisation, evident from the observed range of shell Mg/Ca ratios, we argue that these differences are mechanistically related to the degree of Mg exclusion prior to chamber formation. Indeed, whilst our data for both low-Mg and high-Mg species are consistent with biomineralisation via ions sourced through seawater vacuolisation, it is difficult to reconcile many of these observations with a model based on significant transmembrane Ca transport.

Keywords: foraminifera, biomineralisation, vacuolisation, culturing, Mg/Ca

1. Introduction

Geochemical proxy data from foraminifera forms the basis of much of our knowledge of palaeoceanography and past changes in Earth's climate (e.g. Lear et al., 2000; Elderfield et al., 2012; Rosenthal et al., 2013). Furthermore, this group of unicellular organisms is responsible for a large proportion of oceanic $CaCO_3$ production (Schiebel, 2002), and thus has resulted in a virtually contin-

uous archive of planktonic and benthic species throughout the Cenozoic and beyond. As such, a considerable amount of research has focused on understanding the biomineralisation process in foraminifera (e.g. Erez, 2003; Bentov and Erez, 2006; de Nooijer et al., 2014; Toyofuku et al., 2017; Fehrenbacher et al., 2017). One principal goal of this work is to underpin empirical proxy calibrations between environmental conditions and shell geochemistry with a theoretical basis. Understanding how and why foraminifera modify the chemistry of seawater prior to calcification may improve the accuracy of foraminifera-derived palaeoclimate reconstructions and enable the identification of environmental conditions under which empirical calibrations may require adjustment. For example, the incorporation of Mg in planktonic foraminifera is sensitive to both temperature and the carbonate system (Russell et al., 2004; Evans et al., 2016b; Gray et al., 2018), yet correcting fossil Mg/Ca measurements for secular shifts in ocean carbonate chemistry remains challenging because it is unclear which carbonate system parameter(s) modulate calcification rate and shell Mg uptake (Bach, 2015; Allen et al., 2016; Henehan et al., 2017). Constraining how different foraminifera source and concentrate the inorganic carbon necessary for calcification may address this problem, whilst also providing invaluable information regarding the likely response of this important group of marine calcifiers to ocean acidification.

There is currently no consensus within the community on the fundamental mechanism by which foraminifera source the calcium and carbon necessary for mineralisation, highlighting the challenge of observing and analysing organisms typically less than a millimetre in diameter. Moreover, it indicates that different foraminifera may have evolved different biomineralisation strategies (ter Kuile et al., 1989; de Nooijer et al., 2014), especially between the very diverse benthic

species which produce $CaCO_3$ with a wide range of Mg/Ca ratios and chamber wall structures (e.g. Reiss, 1958; Bentov and Erez, 2006; Evans et al., 2015b; van Dijk et al., 2017). This contribution focuses on the rotaliid (hyaline or perforate) foraminifera, on which most palaeoceanic reconstructions are based.

Direct observation of intracellular processes poses obvious challenges, and as such much recent work has focused on inferences from the isotopic and elemental composition of foraminifera shells (e.g. Segev and Erez, 2006; Zeebe et al., 2008; Raitzsch et al., 2010; Vigier et al., 2015; Evans et al., 2016b). The justification for such studies is a relatively large body of literature on trace element and isotope incorporation into inorganic calcite, which forms the basis of inverse modelling the conditions at the site of calcification. A simple illustration of this is the observation that the Mg/Ca ratio of planktonic foraminifera is approximately twenty times lower than inorganic calcite precipitated from seawater (Mucci and Morse, 1983), providing strong evidence that some species possess a mechanism of excluding Mg before final precipitation of the shell. Based on both direct observation of cellular processes, and inferences such as this, two principal biomineralisation mechanisms have been proposed, briefly summarised here.

(1) The seawater vacuolisation model (SWV), in which ions are predominantly sourced from seawater vacuoles. This model is based on the observation that hyaline foraminifera, in particular *Amphistegina lobifera*, endocytose large quantities of seawater that are transported to the site of chamber formation in vacuoles (e.g. Bentov et al., 2009). Numerous experiments culturing foraminifera in seawater containing membrane-impermeable fluorescent markers such as calcein (623 Da) and FITC-dextran (10 kDa) demonstrates that seawater is present at the site of calcification (e.g. Erez, 2003; Dissard et al., 2009; Evans et al., 2015b). Furthermore,

'pulse-chase' experiments have been conducted by placing foraminifera into seawater containing FITC-dextran or calcein for a period of time, followed by a chase period in normal seawater (Bentov et al., 2009). Material precipitated during the chase period was strongly labelled, demonstrating that the seawater present at the site of biomineralisation must be derived (in part or entirely) from internal seawater vacuoles. Research utilising fluorescent pH indicators has shown that the pH of these vacuoles is increased to ~1 unit above seawater (Bentov et al., 2009; de Nooijer et al., 2009), suggesting that they play an important role in concentrating carbon. Providing support for this is earlier experimental work, using ^{14}C tracer uptake to demonstrate that the hyaline species *A. lobifera* does indeed have a large inorganic carbon pool (ter Kuile and Erez, 1987, 1988). The mechanism of the foraminifera carbon concentrating mechanism was later revealed through confocal microscope observations. Specifically, raising the pH of the vacuole would increase the DIC and $[CO_3^{2-}]$ by promoting CO_2 diffusion directly from acidic vesicles in the cytosol, or possibly from the surrounding seawater (Bentov et al., 2009). Variations of this model invoke vacuole pH elevation through Na^+-H^+ active transport (pumps), which would also modify the vacuole [Li] and δ^7Li given that Na pumps are unlikely to be completely selective for Na^+ over Li^+ (Erez, 2003; Vigier et al., 2015). Therefore, this process may be associated with a minor modification in seawater elemental chemistry. A long-standing challenge of the model is that seawater vacuolisation alone does not explain how many species of foraminifera are able to form calcite shells with a Mg/Ca ratio 1-2 order of magnitude lower than inorganic calcite (e.g. Lea et al., 1999; Erez, 2003; Rosenthal et al., 2011). Therefore, an additional mechanism is required to remove Mg in the seawater vacuolisation model before final precipitation of the shell. This

process has been variously suggested to relate to (i) active Mg removal through channelling and pumping (Erez, 2003; Bentov and Erez, 2006), (ii) uptake by mitochondria (Bentov and Erez, 2006; Spero et al., 2015), (iii) precipitation and removal of Mg-rich phases (Bentov and Erez, 2005; Khalifa et al., 2016), (iv) precipitation through an amorphous or metastable precursor phase (Jacob et al., 2017). Of course, two or several of these processes may act together.

(2) The Ca trans-membrane transport (TMT) model posits that the majority of the calcium required for calcification is channelled and pumped to the site of biomineralisation. The model is based on the example of coccolithophore calcification, in which Ca is indeed channelled and pumped to the calcifying vesicle. In order to explain the higher Mg/Ca ratio of foraminifera compared to coccolithophore calcite and the incorporation of membrane impermeable markers, the model requires a degree of passive seawater transport (Nehrke et al., 2013). It has been argued that this model avoids the requirement for foraminifera to cycle several times their own volume in seawater in order to source calcium exclusively through vacuolisation. For example, an approximately spherical foraminifera 150 μm in diameter has an internal volume of 0.014 ml. In order to precipitate a chamber with a mass of 100 ng it must cycle ~1 ml of seawater in order to source enough calcium. This is ~70 times the volume of the foraminifer, which means that each individual must vacuolise it's own volume of seawater every few hours, assuming chamber formation takes place a few times per week. Proponents of the TMT model argue that this is infeasible, and therefore that some proportion of the calcium must be pumped directly to the calcification site.

Both models require the concentration and conversion of carbon into a form useful for $CaCO_3$ precipitation, given that calcification from seawater is ostensibly

carbon limited ([Ca_{sw}] = 10.3 mM, DIC = ~2 mM). This may be achieved through a carbon concentrating mechanism which creates an internal DIC pool (ter Kuile and Erez, 1987; Erez, 2003; de Nooijer et al., 2009), and diffusion of CO_2 from the cytosol into vacuoles as described above. Recently, in the case of *Ammonia*, it has been suggested that acidification of the foraminifer microenvironment via proton pumping shifts seawater DIC from HCO_3^- to CO_2 (aq), a form that is readily diffused over cell membranes (Toyofuku et al., 2017).

We present new laser-ablation trace element data of two rotaliid foraminifera with contrasting Mg/Ca ratios, the low-Mg planktonic species *Globigerinoides ruber* (white) and the high-Mg benthic *Operculina ammonoides*, grown in modified seawater with variable Mg/Ca ratios and carbonate chemistries. We explore the contrasting control of the carbonate system and temperature on Mg incorporation between these species, and assess a variety of other trace elements (Li, Na, Mn, Sr, Ba) within the context of existing biomineralisation models. Along with a synthesis of data from key experiments conducted over the last few decades, we outline a set of observations that any such model must be able to explain.

2. Methods

2.1. Foraminifera culturing

2.1.1. Operculina ammonoides

Benthic foraminifera were collected from the North Beach, Eilat, Israel at a water depth of 20 m by scuba diving and transported to The Hebrew University of Jerusalem. Live foraminifera were identified as being those that climbed the sides of the container into which they were placed. The culturing procedure for *Operculina ammonoides* is described in detail in Evans et al. (2015b). Briefly, for-

aminifera were cultured in batches of 50 individuals in 150 ml flasks, sealed with a glass stopper and parafilm. Net calcification rates were monitored by twice-weekly measurement of the alkalinity depletion in each culture flask, at which point the seawater was replaced in order to minimise carbonate chemistry change over the course of the experiment. These experiments (denoted DE5) were designed to test the impact of seawater pH and DIC on trace element incorporation. Full details of the carbonate system and trace element chemistry of the experimental seawater are given below and in Tabs. 1 and 2.

The *O. ammonoides* carbonate chemistry experiment consisted of eight cultures, four at (nearly) constant pH (~8.00; DE5-1 – DE5-4) and variable DIC (1525-2357 μM), and four at nearly invariant DIC (~1960 μM; DE5-5 – DE5-8) and variable pH (7.46-8.23 total scale). In order to vary pH and DIC independently of each other, 10 litre batches of natural Gulf of Eilat seawater were diluted from a salinity of 40.65 to 37 psu, acidified to pH ~4, and bubbled with air overnight. The carbonate system of the resulting low-DIC seawater was characterised through alkalinity and pH measurements and then modified to the desired values by titration of Na_2CO_3, HCl and NaOH. The carbonate chemistry of these seawaters was measured again, after which they were immediately syphoned into collapsible, CO_2 impermeable 5 litre bags. The carbonate chemistry of these reservoirs was monitored throughout the experimental period, it is these replicates that the 2SD variability given in Tab. 1 are based. All seawater was labelled with 74 nM ^{135}Ba to enable the unambiguous identification of material precipitated in culture (Evans et al., 2015b).

All *O. ammonoides* cultures took place in temperature-controlled circulating water baths maintained at 25.0±0.3°C. The day/night cycle was approximately

13/11 hours, with a photon flux of ~10 μmol m^{-2} s^{-1} provided by a mixture of natural and artificial light. Previous work has shown that growth rates are reduced when this species is maintained at higher photon fluxes (Evans et al., 2015b). Prior to the initiation of all experiments, foraminifera were placed into natural seawater spiked with 40 μM calcein for 48 hours.

2.1.2. Globigerinoides ruber

Planktonic foraminifera culturing took place at the Interuniversity Institute for Marine Sciences, Eilat, Israel. The procedure for culturing these foraminifera is described in detail in Kisakürek et al. (2008) and Evans et al. (2016a). Briefly, plankton drift tows (without engine power) were conducted at 20 m water depth in the northernmost Gulf of Eilat/Aqaba at a location with a bathymetry of at least 300 m. Foraminifera were immediately picked and separated into individual 120 ml glass culture vessels, placed in temperature-controlled water baths. Culturing took place under a 12 hour light/dark cycle with an irradiance approximately equivalent to that at 20 m open ocean water depth (~400 μmol photons m^{-2} s^{-1}). Foraminifera were fed a juvenile *Artemia* daily until gametogenesis took place, typically less than one week. All vials were sealed with parafilm and a plastic lid to eliminate evaporation and minimise CO_2 exchange with the atmosphere.

These experiments were designed to investigate the effect of the major element composition of seawater on shell Mg/Ca (see Evans et al., 2016a, for a discussion of those data). In the first set of experiments, the seawater Mg/Ca ratio (Mg/Ca_{sw}) was modified between 2.2-6.3 mol mol^{-1} by varying [Mg] (modern open ocean seawater Mg/Ca = 5.2 mol mol^{-1}). An additional set of experiments investigated the effect of temperature at Mg/Ca_{sw} = 3.4 mol mol^{-1}, around 40% lower than natural. Experimental seawater was prepared in large (~10 l) batches in order to

maintain consistency between replicate cultures. Seawater with variable Mg/Ca ratios was prepared by mixing natural seawater with Mg-free artificial seawater made using the recipe of Millero (2013), except for an experiment with Mg/Ca_{sw} higher than modern which was made by spiking natural seawater with $MgCl_2$. As in the *O. ammonoides* cultures, all seawater was labelled with 74 nM ^{135}Ba (5-20× natural) in order to unambiguously identify chambers precipitated in culture. Aside from the Mg/Ca ratio, the elemental chemistry of these artificial/natural seawater mixtures was varied as little as possible. However, as Li was not added to the artificial seawater, the Li/Ca_{sw} ratio varies linearly with the proportion of artificial seawater (Tab. 2). Similarly, Ba/Ca was four times higher in the artificial seawater, presumably as a result of minor impurities in the salts. As far as possible, the carbonate chemistry of these seawaters were invariant (pH 8.0, DIC = ~2100 μM), see Evans et al. (2016b) for details.

2.2. Analytical geochemistry

Upon termination of the experiments, foraminifera were thoroughly washed with distilled water, ultrasonicated, and left in ~3% NaOCl until all organic material had been removed (typically overnight for the larger benthic *O. ammonoides*, 1-2 hours for the planktonic *G. ruber*). Specimens were then ultrasonictaed in 18.2 MΩ deionised water, and rinsed three times. This method is demonstrably effective at removing all NaOCl (see the supplement of Evans et al., 2015b), this cleaning procedure exerts no resolvable impact on measured Na/Ca ratios. Benthic foraminifera were mounted vertically in a pressure sensitive adhesive so that the final chambers precipitated in culture were within 50 μm of the focal plane of the laser. Planktonic specimens were mounted umbilical side-up onto double-sided carbon tape.

All foraminifera were analysed for trace element/Ca ratios using the RESOlution M-50 prototype laser-ablation ICPMS system at Royal Holloway University of London (Müller et al., 2009). Foraminifera analytical details and data quality are described in detail in (Evans et al., 2015a,b) and differed here only in that the Agilent 7500ce ICPMS used in those studies was replaced mid-way through the analytical period with an Agilent 8800 triple-quadrupole ICPMS. All *G. ruber* were analysed using the Agilent 7500ce, whereas *O. ammonoides* from experiments labelled DE5 were analysed using both mass spectrometers. In all cases ablation took place in a He atmosphere (850 ml min^{-1}) with H_2 (8.5 ml min^{-1}) and Ar (~630 ml min^{-1}, optimised daily) added downstream of the ablation cell. H_2 rather than N_2 was used as a diatomic gas in order to reduce the background counts on m/z = 55 by an order of magnitude (Evans et al., 2015b), given that Mn is an element of interest. Fluence was ~3.5 J cm^{-1}, and in all cases a low repetition rate of 2 Hz and short ICPMS sweep time (~0.3 s), along with the 'squid' in-line gas smoothing device, were used in order to maximise vertical spatial resolution through the shell walls. Monitored masses (mass/charge ratios) included ^{7}Li, ^{23}Na, ^{24}Mg, ^{25}Mg, ^{27}Al, ^{43}Ca, ^{55}Mn, ^{88}Sr, ^{135}Ba and ^{138}Ba.

Standardisation was performed by bracketing analyses of NIST SRM612 based on the reported values of Jochum et al. (2011). The only exception to this was Mg/Ca, for which NIST SRM610 was used in the case of *G. ruber* based on the [Mg] of (Pearce et al., 1997), and the MPI-DING komatiite glass GOR132-G (Jochum et al., 2006) in the case of *O. ammonoides*, as this glass is more homogeneous for Mg (Evans et al., 2015b), and has [Mg] far closer to high-Mg benthic foraminifera (NIST612 = 0.0068% Mg, NIST610 = 0.0432%, GOR132-G = 13.5%, *O. ammonoides* = ~3.4%). Data reduction was performed using an

in-house Matlab script. This program subtracts the bracketing gas blank from all analyses, ratios all data to ^{43}Ca, calculates element/Ca fractionation with depth on the glass used for standardisation, and then converts raw ratios into molar ratios based on these (see Longerich et al., 1996). Using this procedure, there is little difference in trace element data quality between the two mass spectrometers, despite a ~4× improvement in sensitivity, as most of the m/z reported here are substantially above the limit of detection. Accuracy and precision are comparable to that previously reported for carbonate analysis at Royal Holloway University of London (see Evans and Müller, 2018). Briefly, based on 27 replicate analyses of the MPI-DING glass GOR128-G analysed over the same analytical period and under identical conditions to the samples: Precision (2SD of all analyses) was <5% for all analytes except B, Zn and Ba (<10%), and accuracy (measured/reported) was <5% except for Zn and Ba (<10%), and Li and Na (11%). Long-term standard analyses indicate that the relatively worse Li and Na accuracy is a result of differential fractionation factors between the MPI-DING and NIST glasses (Evans and Müller, 2018), and is likely an overestimate for carbonate analysis. We do not apply an accuracy correction for this reason.

Seawater samples were analysed for major and trace elements at the NERC Isotope Geosciences Laboratory. Samples were acidified to 1% HNO_3 and 0.5% HCl, and analysed at 30× dilution. Standardisation was performed using three trace element and three major element solutions. Precision (2SD) of element/^{42}Ca ratios based on seven analyses of the certified reference material NASS-4 (seawater) and an in-house seawater standard standard were: ^{7}Li 4%, ^{23}Na 7%, ^{55}Mn 180%, ^{88}Sr 4% and ^{138}Ba 7%. ^{24}Mg/^{42}Ca was an exception to this, instead data quality was assessed using the 20 seawater samples from culturing experiments

in which [Mg] was not modified, as both Mg and Ca behave conservatively in the ocean and this ratio can therefore be assumed to be invariant at 5.2 mol mol^{-1} within analytical precision. Based on these data, Mg/Ca precision was 1%. Accuracy is challenging to assess in seawater elemental data because few reference materials exist with certified trace element values. Na, Mg and Sr/Ca ratios may be compared to open ocean seawater as all of these elements behave conservatively. NASS-4 accuracy assessed in this way is equal to or better than 1% over this analytical session. Li and Mn accuracy cannot be assessed. Measured Ba/Ca of NASS-4 in this study (4.9 μmol mol^{-1}) is comparable to open ocean values (e.g. Lea and Spero, 1994) although this ratio varies considerably, especially as a consequence of freshwater flux and upwelling (e.g. Evans et al., 2015a). Finally, whilst foraminifera Mn/Ca data are discussed below it should be considered that the seawater [Mn] of these samples was close to or below the limit of detection (0.7 ppb). The mean measured Mn/Ca ratio of all seawater analyses (n = 29) is 0.4±0.2 μmol mol^{-1} (2SE), and we use this value for the calculation of distribution coefficients. However, because this value is below the LOD, we stress that the uncertainty in the foraminifera Mn distribution coefficients is much larger than for all other elements and represents a minimum value. Specifically, if [Mn_{sw}] is lower than our measured value, then our *G. ruber* Mn distribution coefficients (Sec. 3.2) would be higher.

2.3. Carbonate chemistry

Alkalinity measurements were performed by Gran titration using a Metrohm 716 DMS Titrino at the Hebrew University of Jerusalem. The titrator was calibrated against NBS pH buffers daily, and long-term total alkalinity measurements were characterised by a reproducibility of ±11 μEq. l^{-1} based on regular analyses

of a certified seawater reference material (Dickson Batch 123, Scripps Institute of Oceanography). The pH of all seawater reservoirs was monitored using an electrode calibrated using NBS buffers. Carbonate system parameters that were not directly measured were determined using co2sys (Lewis and Wallace, 1998), using the same set of constants as (Raitzsch et al., 2010).

3. Results

3.1. Operculina ammonoides Mg/Ca and the carbonate system

Growth rate curves for the different carbonate chemistry experiments, and mean calcite deposited per individual are shown in the supporting material and Tab. 3 respectively. Growth rate, as monitored by alkalinity depletion (i.e. moles $CaCO_3 = (\Delta\mu\text{Eq. l}^{-1} \times V_{culture})/2$), was widely divergent between cultures, as previously observed for *O. ammonoides* (Evans et al., 2015b). Foraminifera in the lowest pH experiment (Tab. 1) were unsurprisingly characterised by the lowest growth rate, however there was otherwise no clear relationship between seawater carbonate chemistry and mean $CaCO_3$ mass added in culture. In part, this likely stems from the limitation of culturing 50 specimens in the same flask, which is necessary in order that the calcification-induced alkalinity depletion is large enough to measure (Δalkalinty over three days was typically 50-100 μEq. l^{-1}). Specifically, it is likely that some specimens did not calcify at all, therefore biasing the mean growth rate per individual for the culture. A possible method of accounting for this is to use the calcein label and ^{135}Ba spike in order to identify the proportion of specimens that precipitated at least one chamber in culture (see the supporting material and below). Normalising the growth data in this way demonstrates a negative impact of pH on calcification (Fig. S2; ($\Delta\mu$g ind^{-1} day^{-1})/(ΔpH) = 334,

$p = 0.07$), but no resolvable effect of seawater DIC.

In total, 516 laser-ablation analyses of *O. ammonoides* from the carbonate system experiments were made (DE5, see Tab. 1). Of these, approximately half (229) were characterized by $^{135}Ba/^{138}Ba$ ratios within error of natural (0.0919) and therefore represent chambers precipitated before the experiments began. Whilst the remainder must have been precipitated in culture, only chambers with mean $^{135}Ba/^{138}Ba$ within error of the ^{135}Ba-spiked culture seawater were used to assess the response of *O. ammonoides* shell chemistry to the carbonate system. This dataset consists of 114 analyses, with an average of 14 and a minimum of 5 from each set of conditions. Based on these data, the response of shell Mg/Ca in *O. ammonoides* to the carbonate system is shown in Fig. 1.

Mg/Ca is weakly positively correlated with pH ($R^2 = 0.43$, $p = 0.08$) over the range 7.46–8.23 (total ion scale). Furthermore, there is no relationship between shell Mg/Ca and DIC; Mg/Ca varies between 144-146 mmol mol^{-1} over the range ~1480–2330 μM (Fig. 1). If DIC exerts any control on Mg/Ca, it is not resolvable in our experiments given that a variation of 2 mmol mol^{-1} is less than the magnitude of the 2SE uncertainty on any measurement.

In contrast, Mg/Ca is significantly positively correlated with $[CO_3^{2-}]$ ($R^2 = 0.63$, $p = 0.02$). Following Bach (2015), the possible control of the culture DIC/H^+ ratio was also investigated (Fig. 1D), with which Mg/Ca is approximately equally correlated. Similarly, although not shown in Fig.1, Mg/Ca is also equally well correlated with $\Omega_{calcite}$, as $[Ca_{sw}]$ was invariant so that this was not decoupled from pH in our experiments. We find no significant relationship between Mg/Ca and alkalinity. Based on these experiments, it is not possible to establish which carbonate system parameter affects Mg incorporation, although DIC and alkalinity

can be ruled out.

There are two significant differences between the response of Mg/Ca to the carbonate system in *O. ammonoides* and low-Mg planktonic species. Firstly, although multiple studies have demonstrated that planktonic shell Mg/Ca is strongly influenced by the carbonate system (Lea et al., 1999; Russell et al., 2004; Kisakürek et al., 2008; Evans et al., 2016b), the relationship is opposite to that which we observe in the high-Mg benthic *O. ammonoides* (Fig. 1). Secondly, in relative terms the control that the carbonate system exerts on Mg/Ca is far greater in planktonic species than in *O. ammonoides*. For example, a combined sensitivity analysis derived from *Globigerinoides ruber*, *Globigerina bulloides* and *Orbulina universa* (Evans et al., 2016b) defines a negative relationship between Mg/Ca and pH with a slope of 7% per 0.1 pH units (or ~3% per 10 μM [CO_3^{2-}] increase). In the high-Mg *O. ammonoides* we observe a ~10% change over the entire studied range of the carbonate system (~0.8 pH units, ~300 μM [CO_3^{2-}]).

3.2. Globigerinoides ruber trace element response to seawater Mg/Ca and temperature

The controls on Mg incorporation into *G. ruber* have been discussed in detail elsewhere (e.g. Nürnberg et al., 1996; Kisakürek et al., 2008; Evans et al., 2016a). Here, we focus on a suite of trace elements (Li, Na, Mg, Mn, Sr and Ba) in cultured *G. ruber* under a variety of seawater Mg/Ca ratios and temperatures (Tab. 4). In particular, we aim to assess whether such data are consistent with calcification from an enclosed reservoir (i.e. Rayleigh fractionation (Elderfield et al., 1996)), and if so, the extent to which this reservoir differs from seawater in composition. The discussion of trace element ratios in these samples must consider the variable trace element composition of the culture seawaters, unavoidable given that

these were composed of mixtures of natural and artificial seawater, as described above. As a result, Li/Ca_{sw} and Ba/Ca_{sw} varied as a function of the proportion of artificial seawater (Tab. 2), which contained no added Li or Ba. Conversely, [Na] and [Sr] were broadly invariant, and [Mn] was at least 5× higher in the artificial seawater (~10 nM) than the Gulf of Eilat, although well within the range of open ocean values (Chester and Stoner, 1974). Therefore, to account for differential trace element concentrations between seawater reservoirs, all trace element data are discussed in terms of their apparent distribution coefficients ($D_x = [X/Ca_{shell}]/[X/Ca_{sw}]$) in the seawater chemistry experiment (i.e. those prefixed 'DE3'; Tab. 2), although the results are also presented here as element/Ca ratios to aid direct comparability.

We observe no relationship between Li/Ca and temperature (Fig. 2A), in line with data from the other symbiont bearing planktonic species *Trilobatus sacculifer* and *Orbulina universa* (Delaney et al., 1985; Hall and Chan, 2004; Allen et al., 2016). Seawater-shell Li/Ca are linearly related under variable $[Li_{sw}]$, and the relationship passes through the origin (Fig. 2F). This implies no relationship between D_{Li} and Li/Ca_{sw}, and therefore that there is a single lithium distribution coefficient under variable $[Li_{sw}]$. This is in partial agreement with the *T. sacculifer* data of Delaney et al. (1985), who observed a linear relationship between seawater-shell Li/Ca, albeit with a positive intercept.

Na/Ca in *G. ruber* is not impacted by temperature or Na/Ca_{sw} over the studied range (Fig. 2B), in agreement with the results of Delaney et al. (1985). However, we note that Na/Ca_{sw} was not varied by experimental design in our cultures. The ±2% range is smaller than analytical uncertainty, likely representing no difference between experiments, and therefore we cannot constrain the impact of Na/Ca_{sw}

on Na incorporation.

It was not possible to assess the relationship between Mn/Ca and temperature, as Mn/Ca was below the LOD by LA-ICPMS in one sample, leaving three samples covering a narrow range (22.5-27.5°C). Similarly, because of the difficulty in measuring [Mn_{sw}] (see Methods) we cannot assess whether seawater-shell Mn/Ca are related in *G. ruber*. However, shell Mn/Ca ratios range between 0.2-2.9 μmol mol^{-1}, and therefore we can confirm that D_{Mn} is >1 in our samples (Tab. 4), as is the case for inorganic calcite (Lorens, 1981; Mucci, 1988).

Sr/Ca is not related to temperature in our cultures, in contrast to the findings of Kisakürek et al. (2008) but in agreement with Allen et al. (2016). The narrow range in Sr/Ca_{sw}, which like Na/Ca, was not varied by design, precludes us from investigating the relationship between seawater-shell Sr/Ca.

Ba/Ca is elevated in the lowest temperature culture, but a possible relationship between Ba/Ca and temperature cannot be determined given (1) this is driven by one data point, and (2) Ba/Ca variability within the temperature experiment is within the range previously reported (Hönisch et al., 2011). We do observe a tightly correlated, positive linear relationship between seawater-shell Ba/Ca (Fig. 2J), characterised by a slope of 0.173±0.027. This is within error of the slope of Hönisch et al. (2011), who found D_{Ba} = 0.15±0.05 by combining data for *G. bulloides*, *G. sacculifer* and *O. universa*. Our data confirm that this relationship is also applicable to *G. ruber*.

4. Discussion: Implications for biomineralisation

4.1. Contrasting Mg incorporation in high and low-Mg foraminifera

Much of the geochemical literature on foraminifera in relation to biomineralisation models focuses on Mg incorporation because of the importance of formulating a mechanistic understanding of the Mg/Ca palaeothermometer, and because many species are able to regulate the Mg/Ca ratio of their shell. Of particular concern is the mechanism by which some foraminifera are able to reduce the Mg content of calcite by more than an order of magnitude compared to inorganic calcite precipitated from seawater (Mucci and Morse, 1983). Hypotheses for how this may be achieved include (1) Mg removal from seawater vacuoles by channels and pumps (Erez, 2003; Bentov and Erez, 2006) and/or uptake by mitochondria (Spero et al., 2015), (2) Ca^{2+} transport to the site of biomineralisation (Nehrke et al., 2013; Toyofuku et al., 2017), and (3) precipitation through an amorphous or metastable precursor phase (Bentov and Erez, 2006; Jacob et al., 2017), although we note that there is no *a priori* reason to suspect that these mechanisms are mutually exclusive. Here, we examine these models in the context of the response of Mg incorporation to both temperature and the carbonate system, contrasting low-Mg planktonic foraminifera with *O. ammonoides*, a high-Mg large benthic species that lacks a mechanism with which to exclude Mg from the site of calcification (Evans et al., 2015b). In fact *O. ammonoides* is characterised by higher Mg/Ca ratios than inorganic calcite, discussed below.

We find that Mg incorporation in low-Mg planktonic species differs from *O. ammonoides* in two fundamental ways. Firstly, as previously described, the slope of the relationship between Mg/Ca and temperature is approximately three to four times lower in *O. ammonoides*, which is characterised by a Mg/Ca in-

crease of 1.8%°C^{-1} (Evans et al., 2013). This is in agreement with studies of other high-Mg benthic species (Toyofuku et al., 2000; Raja et al., 2005; Titelboim et al., 2017), all of which are characterised by a similar slope to inorganic calcite (Oomori et al., 1987). Secondly, Mg uptake in several species of planktonic foraminifera, including *G. ruber*, has been shown to be sensitive to seawater carbonate chemistry (e.g. Lea et al., 1999; Russell et al., 2004; Kisakürek et al., 2008; Evans et al., 2016b). Whether this effect is most appropriately ascribed to [CO_3^{2-}] or pH remains to be determined, but what is clear is that the Mg removal process is substantially less efficient under lower seawater pH and/or [CO_3^{2-}], resulting in higher shell Mg/Ca ratios at lower pH. In contrast, *O. ammonoides* Mg/Ca is relatively insensitive to the carbonate system compared to at least some low-Mg planktonics (Fig. 1), and characterised by a positive relationship between Mg/Ca and pH and/or [CO_3^{2-}].

This comparison is summarised in Fig. 3, alongside relevant inorganic calcite data. The Mg/Ca response to the carbonate system in *O. ammonoides* is in good agreement with the inorganic data of Burton and Walter (1991) if it is considered that the pH at the site of biomineralisation is around one unit higher than the surrounding ambient seawater (Bentov et al., 2009; Toyofuku et al., 2017). The increase in inorganic calcite Mg/Ca with solution pH therefore explains why *O. ammonoides* has a higher shell Mg/Ca ratio compared to calcite precipitated at ambient seawater pH (see also Evans et al., 2015b). Together, these data imply that, in the absence of a mechanism to reduce the calcification site [Mg], as in *O. ammonoides*, the dependency of foraminifera Mg/Ca on the carbonate system conforms to what is known about inorganic calcite (Fig. 3A). Similarly, the relationship between Mg/Ca and temperature in high-Mg benthic foraminifera is

within error of that for inorganic calcite. Overall, this means that biomineralisation models for low-Mg species must be able to explain both the high Mg/Ca-temperature sensitivity, and the Mg/Ca elevation at low pH and/or [CO_3^{2-}], given that this latter feature is demonstrably not an intrinsic feature of calcite precipitation either inorganically or in high-Mg foraminifera.

The mechanism behind the high Mg/Ca-temperature sensitivity in low-Mg foraminifera is unresolved in any biomineralisation model. Hypotheses include: (i) the presence of both very low-Mg and high-Mg secondary/primary phases in foraminiferal calcite, with an increasing proportion of the latter at higher temperatures, proposed by Bentov and Erez (2006) and adopted by (Rosenthal et al., 2011) (which could apply to either the SWV or TMT model), (ii) a decrease in the efficiency of Mg removal at higher temperature, for example if the ability of foraminifera to concentrate carbon increases proportionally faster with increasing metabolic rate (temperature) than their ability to exclude Mg (vacuolisation model), or (iii) an increase in the proportion of seawater leakage to the site of biomineralisation with increasing metabolic rate/temperature (Nehrke et al., 2013) (TMT model). Given that our data do not constrain the mechanism of the sensitivity of Mg/Ca to temperature, we focus on examining whether these explanations can be reconciled with our observations of the response of shell Mg/Ca to the carbonate system (Fig. 3).

In the vacuolisation model, the efficiency or degree of Mg exclusion increases with increasing pH and/or [CO_3^{2-}], see Fig. 3B. Evans et al. (2016b) hypothesised that this process may become less efficient under conditions unfavourable for calcification, as increased energy expenditure on modifying the carbonate chemistry of the vacuole is necessary to source the carbon required for calcification. Conse-

quently, the foraminifer has fewer resources with which to channel or complex Mg away from the site of calcification. Indeed, Zeebe and Sanyal (2002) show that H^+ removal is a more effective strategy than Mg^{2+} removal when precipitating calcite from seawater. It follows that under conditions less favourable for calcification (i.e. low pH or low $[CO_3^{2-}]$), foraminifera may prioritise H^+ removal. Alternatively, whilst Mg may be channelled down the concentration gradient between a seawater vacuole and the cytosol ([Mg] = 1-2 mM), excess Mg may eventually need to be removed from the cell. If the efficiency of this depends on the ambient seawater-cytosol pH gradient, then the rate at which Mg can be removed may be sensitive to seawater carbonate chemistry. Irrespective of the mechanism, we can exclude inorganic processes as the cause given that we find no such relationship between Mg/Ca and the carbonate system for high-Mg foraminifera (Fig. 3A).

Conversely, if the primary purpose of vacuolisation is to feed on microorganisms (Nehrke et al., 2013), then the TMT model must also be able to explain why it is beneficial (or unavoidable) for foraminifera to increase their metabolic rate at lower pH or $[CO_3^{2-}]$. Unlike temperature, there is not a clear reason for doing so in response to the carbonate system, particularly given that Toyofuku et al. (2017) argue that the proton flux associated with calcification is independent of seawater carbonate chemistry (i.e. the low-Mg *Ammonia* is characterised by equivalent proton fluxes at low and ambient pH). We argue that taken together, this observation, and the data summarised in Fig. 3, demonstrate that variation in shell Mg/Ca in response to temperature and the carbonate system is not a passive process driven by metabolic rate. Rather, Mg removal is an active process, the efficiency of which is impacted by a number of factors including temperature and the carbonate system. We do not mean to imply that there are no inter-species differences in biomineral-

isation. Indeed it is evident both from our data, and many previous observations (e.g. Bentov and Erez, 2006), that the widely varying shell Mg/Ca ratios of different foraminifera call for widely varying degrees to which the seawater Mg/Ca ratio at the site of biomineralisation is reduced. Nonetheless, we find that the response of shell Mg/Ca to the carbonate system and Mg/Ca_{sw} in several species of low-Mg planktonic foraminifera is difficult to reconcile with the TMT model, because it is not clear why more seawater would be vacuolised when the ambient pH is lower if this is a passive process. By implication, we argue that the inter-species differences in biomineralisation mechanism are principally related to the degree to which Mg is removed from the calcifying space, with no need to invoke TMT in any hyaline foraminifer.

We note that the low-Mg benthic foraminifera are apparently an exception to the above discussion, in that some species are characterised by a positive relationship between shell Mg/Ca and $\Delta[CO_3^{2-}]$, i.e. opposite to the low-Mg planktonics (e.g. Elderfield et al., 2006; Rosenthal et al., 2006; Yu and Elderfield, 2008; Bryan and Marchitto, 2008). Whilst we lack the data to demonstrate unambiguously why this is the case, it may be that this discrepancy results from early diagenetic preferential loss of higher-Mg components of the shell in bottom waters with low or negative $\Delta[CO_3^{2-}]$, although an alternative mechanism related to the calcification process of these foraminifera has been proposed (see Bryan and Marchitto, 2008). Nonetheless, preferential dissolution of higher-Mg components has been shown to be the process by which the Mg/Ca ratio of planktonic foraminiferal calcite may be biased (Fehrenbacher and Martin, 2014; Johnstone et al., 2016). Indeed, no significant relationship between $[CO_3^{2-}]$ and Mg/Ca was found in cultured *Ammonia tepida* (Dissard et al., 2010). However, whilst the positive Mg/Ca-$\Delta[CO_3^{2-}]$

relationship observed in core-top samples of some low-Mg benthic species may be a secondary feature, the absence of a relationship between Mg/Ca and $[CO_3^{2-}]$ in cultured specimens is different to both most planktonics and the high-Mg benthic *O. ammonoides* (Fig. 3). It could be that the low-Mg benthics, which inhabit environments that are broadly less saturated than the surface ocean (the deep ocean) and/or less stable (e.g. tidal or estuarine settings), are better adapted to calcification from seawater with a lower $[CO_3^{2-}]$. In addition, a relatively less efficient mechanism for Mg removal in low-Mg benthics from less saturated seawater could be balanced by an overall lower rate of chamber addition, whereas planktonic foraminifera may prioritise chamber formation rate over the reduction of the shell Mg/Ca ratio.

4.2. Trace element incorporation into G. ruber

Consensus exists on the presence of seawater at the site of biomineralisation in foraminifera, based on the observation that membrane-impermeable dyes are incorporated into the shell (e.g. Erez, 2003; Bernhard et al., 2004; Bentov et al., 2009; Evans et al., 2015b; Nehrke et al., 2013). Furthermore, the trace element composition of foraminiferal calcite differs greatly from that of coccolithophores (Müller et al., 2011), which source Ca through TMT (e.g. Sviben et al., 2016). Given these robust observations, it is a common feature of both the SWV and TMT models that precipitation takes place from compositionally modified seawater.

Following this logic, we ascertain the degree to which the Mg/Ca ratio of the calcifying fluid must be modified relative to seawater by utilising data from inorganic calcite precipitation experiments. Calcite precipitated at a pH similar to that of the calcification site (i.e. ~9; Bentov et al. (2009)) has a Mg/Ca ratio of ~140 mmol mol^{-1} (Burton and Walter, 1991), see Fig. 3A, which is around 35 times

higher than low-Mg foraminifera such as *G. ruber*. de Choudens-Sánchez and González (2009) compiled Mg/Ca data from inorganic precipitation experiments under variable solution Mg/Ca ratios. Based on these data, the best fit power relationship between the Mg distribution coefficient and seawater Mg/Ca in inorganic precipitation experiments is:

$$D_{Mg} = 0.0425 \times Mg/Ca_{sw}^{-0.4808} \quad (1)$$

Using a calcite Mg/Ca ratio of 4 mmol mol^{-1} in low-Mg foraminifera, this implies that the Mg/Ca ratio of the modified seawater at the site of biomineralisation is <0.1 mol mol^{-1}, or >50 times lower than seawater. Specifically, a measured Mg/Ca_{shell} of 4 mmol mol^{-1} requires Mg/Ca_{sw} to be 0.0105 mol mol^{-1}, i.e. from equation 1, $D_{Mg} = 0.0425 \times 0.0105^{-0.4808} = 0.38$, so that $Mg/Ca_{shell} = 0.38 \times 0.0105 \times 1000 = 4$. To achieve this, foraminifera would need to increase the biomineralisation site [Ca] by a factor of 500, to ~5 M. However, we note that the application of these inorganic data to foraminifera with relatively very low $Mg/Ca_{calcite}$ ratios is uncertain and therefore this may represent a worst-case end-member. Nonetheless, even if we take the inorganic calcite D_{Mg} of 0.02 in normal seawater (Mg/Ca = 5.2 mol mol^{-1}) and assume that it does not vary as a function of Mg/Ca_{sw}, a best case scenario given that there is abundant evidence that this is not the case (de Choudens-Sánchez and González, 2009), this would still imply a [Ca] in the calcifying space 25× higher than seawater.

The disagreement between these calculations and those presented in the original description of the TMT model arise because Nehrke et al. (2013) did not consider that Mg is highly incompatible (D_{Mg} = ~0.02, see Eq. 1 and compare with Eq. A3-5 of Nehrke et al. (2013)). As a result, the percentage of ions arriving by passive transport is incorrect by a factor of 50 even within the constraints of the

TMT model. Irrespective, we consider a Ca concentration factor of 25-500 relative to seawater (see above) to be unrealistic for two reasons. Firstly, the extreme saturation state implied by a [Ca] far in excess of seawater means that foraminifera would be unable to concentrate DIC into the calcifying space, and spontaneous precipitation may occur long before that [Ca] could be achieved (note that coccolithphores, which do transport Ca, achieve this by storing Ca as a disordered Ca-P precursor phase (Sviben et al., 2016)). Second, a greatly increased [Ca] is inconsistent with observations of the apparent distribution coefficients for most other trace elements in the shells of foraminifera. Specifically, if such Ca enrichment were possible at the calcification site, then the concentration of trace elements in the foraminifera shell would be orders of magnitude lower than inorganic calcite because of the greatly reduced solution trace element/Ca ratios as a result of Ca concentration.

In order to illustrate this second argument, the *G. ruber* trace element data (Fig. 2, Tab. 4) is interpreted in terms of a simple Rayleigh fractionation model in Fig. 4, following Elderfield et al. (1996) and Dawber and Tripati (2012). The purpose of this exercise is to assess the first-order effect exerted on apparent trace element distribution coefficients by possible Ca transport to the site of biomineralisation. We stress that these simple models do not capture or explain the complexities of trace element incorporation (see e.g. Erez, 2003; Eggins et al., 2003; Spero et al., 2015). Whilst they are useful as tools to assess the role of Ca transport and approximate degree of Ca utilisation, our intention is not to explain the detail of any trace element system through Rayleigh fractionation alone.

To assess the *G. ruber* trace element data in this context, knowledge of inorganic calcite partition coefficients is required. We use distribution coefficients

from Mg-free inorganic precipitation studies, in order to mirror the assumption that $Mg/Ca_{sol.}$ is lowered before calcite precipitation in foraminifera takes place, consistent with both biomineralisation models. Specifically: $D_{Li} = 1.05\times10^{-4}$ from experiment 'Li-1' of Okumura and Kitano (1986) based on the initial [Ca] of that experiment ([Ca] decreased as precipitation progressed). Although we also consider that given by Marriott et al. (2004) ($D_{Li} = 0.00382$), we do not use this value in our calculations as the method used to precipitate calcite in that study resulted in highly saturated conditions ($[Ca_{sol.}] = 240$ mM), with a likely strong influence on growth rate. $D_{Na} = 1.0\times10^{-4}$ (interpolated from the two experiments of Ishikawa and Ichikuni (1984) with solution Na/Ca ratios closest to seawater). $D_{Mn} = 30$ (Lorens, 1981). $D_{Sr} = 0.13$, from the intercept of the D_{Sr}-$Mg/Ca_{calcite}$ relationship given by Mucci and Morse (1983), which has been shown to be applicable to foraminiferal calcite (Evans et al., 2015b). $D_{Ba} = 0.08$ (Kitano et al., 1971). An additional source of uncertainty in this exercise is that trace element incorporation is dependent on other factors, particularly growth rate (e.g. Mucci and Morse, 1983). We add an arbitrary ±10% uncertainty to the inorganic distribution coefficients in order to examine how an uncertainty of this magnitude would affect our interpretation of the *G. ruber* data (Fig. 4). In some cases this is likely to be an underestimate, but we again stress that this exercise is designed only to assess whether the data are broadly compatible with Rayleigh fractionation in the context of different biomineralisation models.

Rayleigh fractionation modelling of trace element incorporation into *G. ruber* assuming no Ca transport to the site of biomineralisation (the first column of panels in Fig. 4) demonstrates that all of the investigated trace elements are broadly explicable by the seawater vacuolisation model, with the possible exception of

Li. Elements with widely different distribution coefficients in inorganic calcite are consistent with *G. ruber* calcite precipitation from a closed pool similar to seawater, and Ca utilisation fractions of ~20-90%. This finding is also consonant with previous estimates based on benthic foraminifera (Elderfield et al., 1996; Dawber and Tripati, 2012). Notably, the results of the first study to use this approach show that Rayleigh fractionation can also explain the incorporation of Cd into foraminifera (Elderfield et al., 1996). Together with our Mn and Na data, this demonstrates that the predictions of these simple models are consistent with trace elements that have distribution coefficients both greater and less than unity.

The minor disagreement between different trace elements in terms of the implied degree of calcium utilisation (Fig. 4) likely stems from at least three complications. As highlighted above, trace element incorporation depends on growth rate, but also solution carbonate chemistry in both inorganic and foraminiferal calcite (e.g. Burton and Walter, 1991; van Dijk et al., 2017). The major ion chemistry of the solution is an additional factor that must be considered, for example, the covariance of Mg and Sr (Mucci and Morse, 1983), or the competition between alkali elements (Okumura and Kitano, 1986). Given that most inorganic calcite studies are not performed in seawater, the inorganic calcite distribution coefficients that we use may be differ from those at the site of biomineralisation in foraminifera. Interestingly, it is difficult to reconcile Li/Ca ratios in foraminifera with what is known about inorganic calcite D_{Li}, unless the presumably rapidly precipitated inorganic experiments of Marriott et al. (2004) are applicable to these organisms (Fig. 4). Foraminiferal [Li] is about an order of magnitude higher than in the precipitation experiments of Okumura and Kitano (1986), which were conducted with a $[Ca_{sol.}]$ similar to seawater. It is beyond the scope of this study to

address this issue in detail, except to note that Li has been implicated in the mechanism by which foraminifera modify the carbonate chemistry of seawater vacuoles (Vigier et al., 2015). The high concentration of Li is consistent with the use of a Li-proton pump to modify the pH of vacuolised seawater in order to promote DIC accumulation through CO_2 diffusion into the alkaline vacuoles. If this hypothesis is correct, it may not be surprising that Li, like Mg, cannot be interpreted solely in terms of Rayleigh fractionation even to a first-order approximation.

Despite these complications, we demonstrate that the majority of commonly measured trace elements are consistent with closed-system precipitation from seawater with an unmodified calcium concentration, and therefore with the vacuolisation model of foraminifera biomineralisation (Fig. 4). In addition, despite some offsets between the calculated fraction Ca utilised between trace element systems, likely derived from the reasons described above, comparing the degree of Ca utilisation between systems (Fig. S3) demonstrates that several are correlated, most notably Na-Sr-Ba. This strongly argues for Rayleigh fractionation as one of the primary controls on trace element incorporation into *G. ruber*. Given these observations, the question is then whether these data can also be reconciled with the TMT model.

The TMT model demands a significant degree of cellular Ca transport into the calcifying space, which is presumably composed of a very small proportion of 'leaked' seawater (~1%), possibly with a major cytosol component (Nehrke et al., 2013); cytosol differs from seawater in that the concentration of Na, Mg, and especially Ca, are far lower. Typical intracellular ionic Ca, Mg and Na concentrations are <1 μM, ~1 mM and ~0.1 M respectively (Romani and Maguire, 2002). Therefore, it follows that the concentration of these elements may also be

lower at the site of biomineralisation compared to seawater in this model. However, in the absence of any measurements of the composition of the fluid at the site of biomineralisation, we assume that this transport occurs into a space filled with a fluid equivalent to seawater. Although this may not necessarily be the case in the context of TMT model, our calculations represent a best-case scenario in terms of reconciling observed foraminifera trace element distribution coefficients with TMT, given that lower concentrations of these elements in the cytosol would push apparent shell distribution coefficients even further from inorganic calcite precipitated from seawater. Rayleigh fractionation models with differing components of Ca transport are shown in the second two columns in Fig. 4.

An additional consideration is that Ca channels may be poorly or non-selective for Sr^{2+} and Ba^{2+} (Allen and Sanders, 1994), unlike Mg^{2+}. It has been shown that coccolithophore Sr/Ca and Ba/Ca ratios are consistent with a poorly-selective Ca channel and inorganic calcite distribution coefficients (Langer et al., 2009), which also provides an explanation for the broadly comparable Sr/Ca and Ba/Ca ratios between foraminifera and coccolithophores. For this reason the D_{Sr} and D_{Ba} panels in Fig. 4 display model endmember scenarios assuming both non-selectivity and complete selectivity. If Ca channels are poorly selective, these trace elements cannot provide a good test of the TMT model.

In contrast, Ca channels are known to be highly discriminative against Na^{+} and Mg^{2+} (McCleskey and Almers, 1985; Sather, 2005), whereas Mn^{2+}, which has a similar radius/charge ratio as Ca^{2+} in solution, may be variably transported depending on the type of calcium channel (Aoki et al., 2002; Felder et al., 1994). In the absence of any data regarding the selectivity of Ca channels in foraminifer, the Rayleigh fractionation models for Li, Na, and Mn at $2\times[Ca_{sw}]$ and $10\times[Ca_{sw}]$

(Fig. 4) assume negligible transport of these elements.

Overall, this exercise demonstrates that significant Ca transport to the site of biomineralisation would mean that it is not possible to reconcile the observed Mn and Na distribution coefficients of *G. ruber* with each other, or with the alkali earth elements. Specifically, D_{Mn} >1 requires very low degrees of Ca utilisation (<10%) if the biomineralisation site [Ca] is 10 times higher than seawater. In contrast, the observed D_{Na} would require the opposite, namely extremely high or impossible degrees of utilisation even at [Ca] double that of seawater. Although we illustrate 2× and 10× [Ca_{sw}] in Fig. 4, we note that if the low Mg/Ca ratio of foraminifera is explained entirely through Ca transport, far higher degrees of Ca concentration than the range explored with these models would be required (see above), which would result in an even less favourable comparison between trace elements. The TMT models shown in Fig. 4 could also be considered a best-case scenario, accounting for the possibility that the biomineralisation site may not be a completely closed system, and if a cytosol component is present at the biomineralisation site.

Whilst it may be the case that foraminifer Ca channels are poorly selective for elements other than Sr and Ba, this cannot be so for Na, given that there would be little benefit of such a channel operating in seawater. Similarly, even if these channels were poorly selective for Mn, it would be difficult to reconcile the very low degrees of Ca utilisation implied by our observed D_{Mn} compared to those based on Sr and Ba. Based on these data we argue that the TMT model cannot explain why the Na/Ca, Mn/Ca and Cd/Ca ratios at the site of biomineralisation are similar to seawater. Unless foraminifera Ca channels are shown to be nonselective for all of these elements then the trace element content of low-Mg foraminifera means that

significant Ca transport is unlikely. Finally, although our models are based solely on *G. ruber*, we note that many other low-Mg species have broadly comparable trace element/Ca ratios (e.g. Delaney et al., 1985; Allen et al., 2016), demonstrating that the implications of this exercise hold true for many other foraminifera.

4.3. Seawater vacuolisation

Although several studies have demonstrated the presence of internal Ca and carbon pools in at least some benthic foraminifera (ter Kuile and Erez, 1987, 1988; Erez, 2003), it has been suggested that seawater vacuolisation cannot source the ions necessary for calcification even if this process is taken into account, especially in species with no resolvable internal pool (Nehrke et al., 2013). Specifically, it has been argued that the vacuoles observed in foraminifera are not sufficiently large or numerous to source the required Ca^{2+}, and therefore that a significant proportion must be transported, providing evidence for the TMT model.

We offer two lines of evidence demonstrating that seawater vacuoles can source Ca quickly enough for calcification without the need for additional transport. Firstly, we provide new images of seawater vacuolisation in the intermediate-Mg benthic foraminifera *Amphistegina lessonii* (Fig. 5), chosen to illustrate that seawater vacuoles in foraminifera are both large and numerous. Fluorescent confocal microscopy images of live specimens in a pulse-chase experiment are shown in Fig. 5A-B. Here, several specimens were placed into calcein-labelled seawater for several hours, then washed with unlabelled seawater and transferred into a petri dish. The shell is not fluorescent because no precipitation took place in this short interval, but fluorescence is visible in many of the chambers, and individual vacuoles can clearly be seen even through the chamber wall. In the specimen shown in Fig. 5A, approximately half of the volume of the foraminifera consists

of seawater vacuoles, a common feature of our observations of both *A. lessonii* and *O. ammonoides*.

Seawater vacuoles are shown under greater magnification in Fig. 5C-D. These images are clearer because this is a partially dissolved specimen (see Bentov and Erez, 2005, for methodology). Briefly, a decalcified foraminifera (using EDTA) is transferred to seawater where it forms a 'recovering individual' that may attach to the glass as it begins to re-calcify. As in the whole specimens described above, the cytoplasm is largely composed of a large quantity of rapidly moving seawater vacuoles, visible both with and without calcein labelling. A similar proportion of vacuoles are observed in both intact specimens (Fig. 5A) and recovering individuals (Fig. 5C), demonstrating that the vacuoles observed in recovering individuals is not an unrepresentative response to shell dissolution. Whether or not planktonic foraminifera are also characterised by an abundance of internal vacuoles remains to be demonstrated, but we show that seawater is also present at the calcification site (Fig. 5E), and at least some foraminifera have sufficient vacuoles to source the ions required for calcification through this mechanism.

A further compelling argument that foraminifera are capable of calcification without significant Ca transport is that there are many hyaline foraminifera with a Mg/Ca ratio equivalent to or greater than inorganic calcite (we do not consider the miliolid foraminifera here, which likely calcify by a different mechanism (e.g. ter Kuile et al., 1989)). These include the genera *Planoglabretella* (Toyofuku et al., 2000), *Heterostegina* (Raitzsch et al., 2010) and *Operculina* (Evans et al., 2013), see Fig. 3. Proponents of the TMT model argue that Ca-transport explains the low Mg/Ca ratio of many foraminifera compared to inorganic calcite. Therefore, it follows that there cannot be significant Ca transport in species which have a

Mg/Ca ratio similar to, or higher than, inorganic precipitates. The possibility that calcification occurs through an amorphous precursor phase does not bear on this observation, given that experimental evidence shows that ACC transformation to calcite does not change the Mg/Ca ratio (Blue et al., 2017). We argue that these high-Mg foraminifera provide robust evidence that large chambers can be precipitated without the need for significant Ca transport. Therefore, it must be possible for vacuoles to be cycled at a high enough rate in order to source sufficient Ca for calcification, and there is no evidence to suggest that planktonic or deep-benthic species are different in this respect.

The seawater vacuolisation model demands that foraminifera are able to cycle several times their own volume in seawater every day. For example, a large planktonic foraminifera 350 μm in diameter that precipitates a chamber with a mass of 2 μg twice per week (see the size-mass relationship of Henehan et al. (2017)) would need to cycle ~15 times its volume per day. The larger benthic foraminifera *O. ammonoides* (0.5 mm diameter, precipitating at an average rate of ~4 μg $CaCO_3$ day^{-1}, Tab. 3) would need to cycle seven times it's volume. Our observations of vacuolisation in foraminifera are consistent with this, namely a significant proportion of the shell volume is indeed composed of seawater vacuoles (Fig. 5), with a residence time in the order of an hour (see Bentov et al., 2009).

Lastly, it has been argued that if seawater vacuoles play a passive role in biomineralisation, then seawater and shell Mg/Ca should be linearly related (Nehrke et al., 2013). Whilst it is the case that the data of Segev and Erez (2006), based on EPMA measurements of *Amphistegina*, are within error of a linear relationship, a power curve through these data provides a slightly better fit. More recently, careful culturing work has utilised labels incorporated into the shell (such as calcein

or a ^{135}Ba isotope spike), so that new growth can be unambiguously identified by spatially resolved analysis. Seawater-shell Mg/Ca measurements based on these techniques demonstrates that this relationship is nonlinear for both high-Mg and low-Mg foraminifera (Raitzsch et al., 2010; Evans et al., 2015b, 2016a), and it has been argued that this is a general feature of marine calcifiers (Hasiuk and Lohmann, 2010). Given that several of these experiments were conducted in seawater with variable [Mg] but constant [Ca], it is difficult to see why a greater proportion of vacuoles would be transported at lower than present-day seawater Mg/Ca. The clear prediction of the TMT model, namely that shell and seawater Mg/Ca should be linearly related therefore requires further scrutiny. We note that there is growing indirect evidence that this is also the case for low-Mg deep benthic foraminifera (Evans and Müller, 2012; Lear et al., 2015; Evans et al., 2016a).

5. Conclusions

Calibrating the relationship between foraminifera shell chemistry with all environmental factors that have undergone secular variation over geological time may represent an insurmountable challenge for the palaeoceanographic community. Given the biological and geochemical overprint that these processes exert on trace element and isotope systems in these tightly biologically-mediated calcites, developing a mechanistic understanding of the biomineralisation process is of fundamental importance.

At present, there is no consensus of whether foraminifera dominantly source the Ca required for chamber formation through seawater vacuolisation or transmembrane transport, or indeed if all hyaline foraminifera utilise the same mechanism (de Nooijer et al., 2014). Here, we present laboratory culture data of both

Operculina ammonoides and *Globigerinoides ruber* and highlight several observations and features of trace element incorporation that any biomineralisation model must be able to accommodate. Specifically:

1. Mg incorporation in many low-Mg foraminifera is highly sensitive to the carbonate system, which is not the case for high-Mg foraminifera (Fig. 3).
2. Low-Mg foraminifera have Na, Mn, Sr, Cd and Ba/Ca ratios consistent with inorganic calcite precipitation from slightly modified seawater (high pH and DIC, but ~10 mM [Ca]) in a (semi) enclosed pool (Fig. 4).
3. Some species, such as *A. lobifera* possess large internal Ca pools (Erez, 2003).
4. At least some foraminifera vacuolise large quantities of seawater (Fig. 5A-D), and all species that have been tested are labelled with membrane-impermeable fluorescent dyes. This includes planktonic foraminifera (Fig. 5E), and provides direct evidence for seawater at the site of calcification.
5. Foraminifera tightly control the carbonate chemistry of vacuolised seawater.
6. The balance of evidence is that the relationship between shell and seawater Mg/Ca is nonlinear in all species studied so far.

Whilst we stress that there may be important inter-species differences in biomineralisation mechanisms, most clearly evident in the range of observed shell Mg/Ca ratios, we argue that all of these observations are consistent with a biomineralisation model centred on seawater vacuolisation. Specifically, precipitation takes place from seawater, with the large inter-species range of shell Mg/Ca entirely explicable through differences in the degree to which the [Mg] of the calcifying fluid is mediated. This may occur through Mg channels, complexation, a metastable precursor phase (Jacob et al., 2017), and/or uptake into mitochondria (Bentov and

Erez, 2006; Spero et al., 2015). Moreover, Rayleigh fractionation modelling indicates that the concentration of [Ca] (and all other ions except for Li and Mg) at the biomineralisation site cannot be significantly different from seawater, unless foraminifera Ca channels are non-selective for all of the trace elements investigated here. We consider this to be highly improbable. Furthermore, the seawater vacuolisation model can explain the divergent response of Mg to the carbonate system in low and high-Mg species, if the mechanism by which Mg is removed competes energetically with the need to modify the carbonate chemistry of seawater vacuoles. Finally, it explains the large amount of seawater vacuoles observed in at least some species (e.g. Fig. 5; Bentov et al. (2009)).

In contrast, it is difficult to see how all of these observations can be accommodated into the TMT model. For example, whilst Ca channels may be poorly selective for Sr, the observed Na/Ca ratios of low-Mg foraminifera would require that Ca channels transport ~45× more Na than Ca in order to maintain a biomineralisation site Na/Ca ratio similar to seawater. Shell Mg/Ca is nonlinearly related to seawater Mg/Ca in all high and low-Mg species investigated so far, which is challenging to explain through seawater transport. Moreover, it is not clear why foraminifera would expend energy on modifying vacuole carbonate chemistry if they play a passive role in biomineralisation (compare Bentov et al. (2009) and Toyofuku et al. (2017)). Finally, we argue that the existence of hyaline species with a Mg/Ca ratio not resolvably distinct from inorganic calcite (e.g. *O. ammonoides* and *H. depressa*) demonstrates that foraminifera must be able to source the Ca required for chamber formation without transport, as to do so would lower the shell Mg/Ca ratio.

The foraminifera are a hugely diverse and ancient group of organisms, raising

the likelihood that there is no universal method by which all species calcify. The diversity of shell chemistry (e.g. Bentov and Erez, 2006), divergent responses to laboratory acidification (Fujita et al., 2011; Henehan et al., 2017), and large variation in the relative size of internal Ca pools (Erez, 2003; Nehrke et al., 2013) indicate that this is indeed the case. Nonetheless, the features that we highlight above are common to many low and high-Mg species, and any biomineralisation model must be able to accommodate them.

Acknowledgements

We are grateful to Shai Oron (IUI, Eilat) for help with sample collection, and to Tom Barlow and Simon Chenery (BGS, UK) for ICPMS trace element analysis of seawater samples. LA-ICPMS work at RHUL was co-funded by SRIF3 (HEFCE) and NERC (NERC CC073) equipment grants. We would like to thank the editor and reviewers for their time and constructive comments, which greatly improved this contribution.

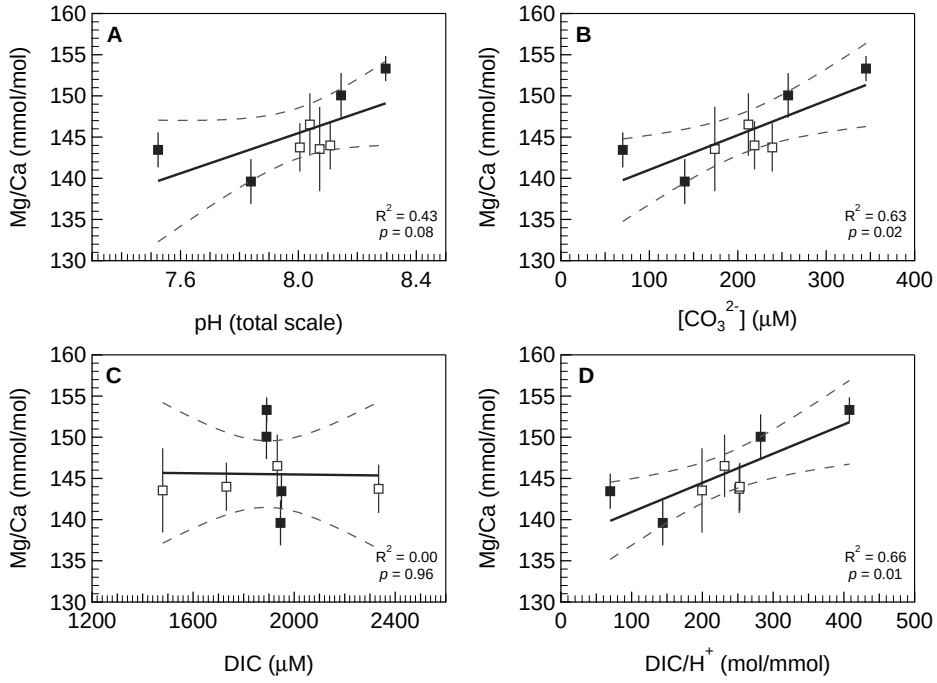

Figure 1: The relationship between Mg/Ca and the carbonate system in laboratory cultured *Operculina ammonoides*. Black squares represent experiments with approximately invariant DIC but different pH, white squares are experiments at approximately the same pH but variable DIC. Mg/Ca error bars are 2SE. In all cases the regressions are based on data from all experiments.

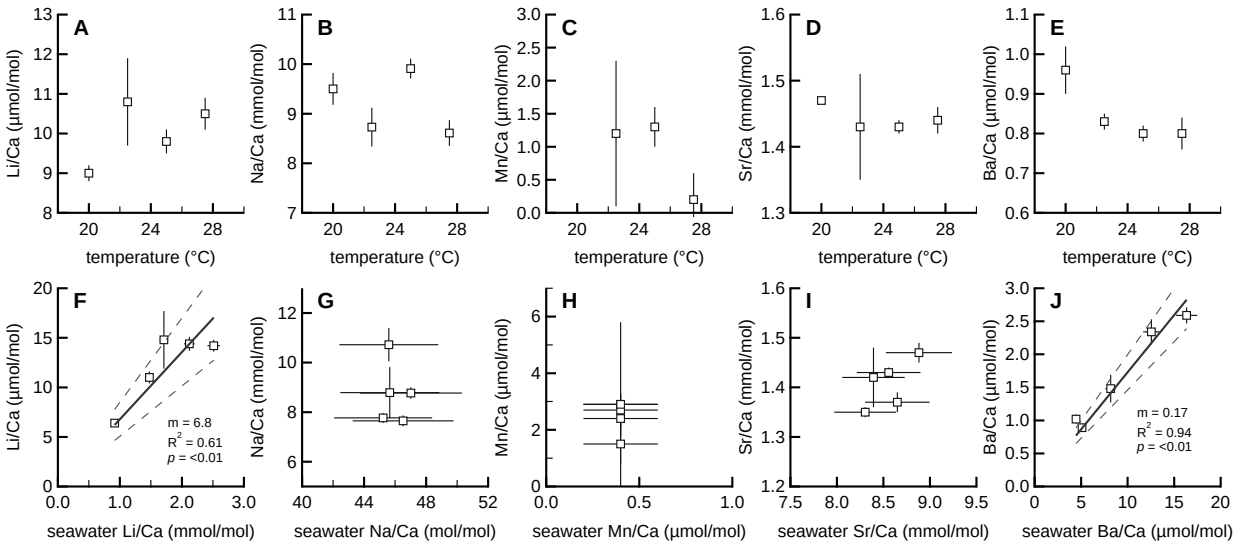

Figure 2: The control of temperature and seawater chemistry on trace element incorporation in cultured *Globigerinoides ruber*. All cultures were performed in mixtures of artificial and natural seawater, with the primary aim of varying the seawater Mg/Ca ratio (see Tab. 2). Because some trace elements were not added to the artificial seawater (e.g. Li, Ba), this resulted in variability in the concentration of these as a function of the proportion of artificial seawater. All temperature experiments were carried out at a Mg/Ca_{sw} ratio ~60% of modern. See Evans et al. (2016a) for a detailed analysis of the Mg/Ca data, which is not repeated here.

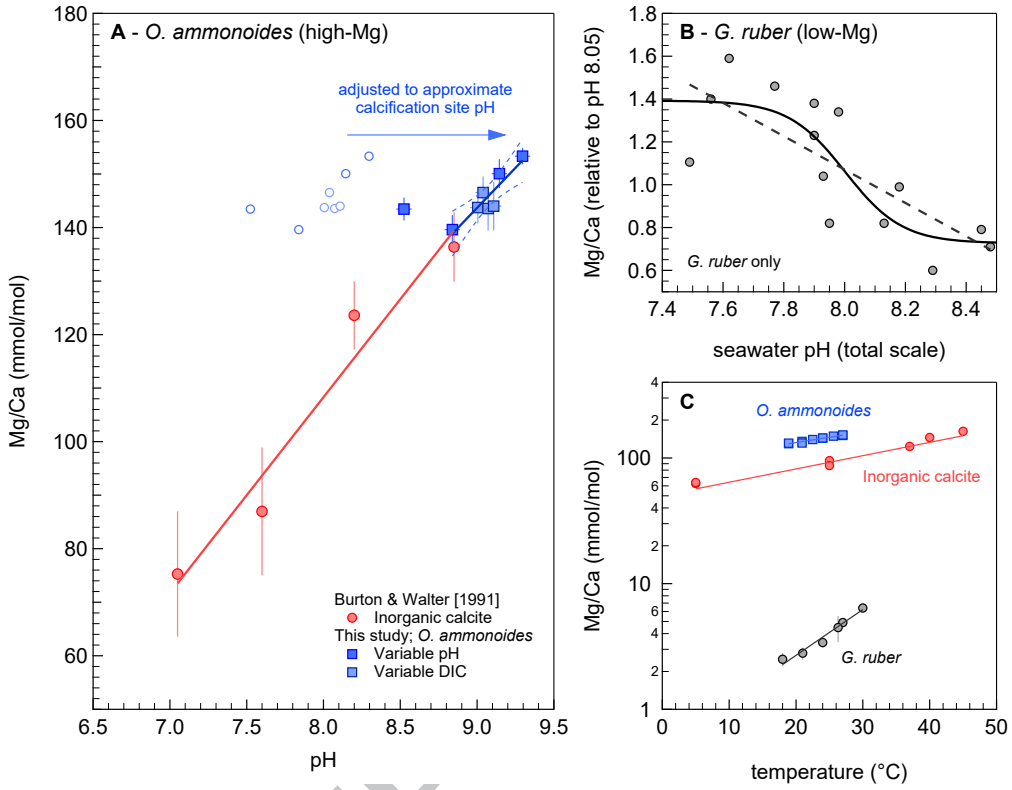

Figure 3: The contrasting dependency of Mg incorporation on the carbonate system and temperature in low and high-Mg foraminifera. (A) *Operculina ammonoides* Mg/Ca response to seawater pH, compared to inorganic calcite precipitated from seawater (Burton and Walter, 1991). The foraminifera data are shown as in Fig. 1 (open blue circles), as well as adjusted to the calcification site pH (closed blue squares), assuming this is 1 unit above ambient seawater (see text). The regression through the foraminifera data excludes one data point, see Fig. 1 for the equivalent regression including all data. (B) *Globigerinoides ruber* Mg/Ca response to pH, modified from Evans et al. (2016b) to include the data given in Allen et al. (2016). Both a linear and logistic function are fitted through all the data, the latter of which captures the lower sensitivity of planktonic Mg/Ca to the carbonate system at pH and/or [CO_3^{2-}] extremes (see Russell et al., 2004; Evans et al., 2016b). The response of Mg incorporation to pH in planktonic species over the range ~7.7 to 8.2 is in the opposite direction and of a much larger relative magnitude compared to high-Mg benthics. (C) Comparative Mg/Ca-temperature relationships in both high/low-Mg species (Evans et al., 2015b; Kisakürek et al., 2008), compared to inorganic calcite (Oomori et al., 1987). Note the logarithmic scale to facilitate comparison of slopes.

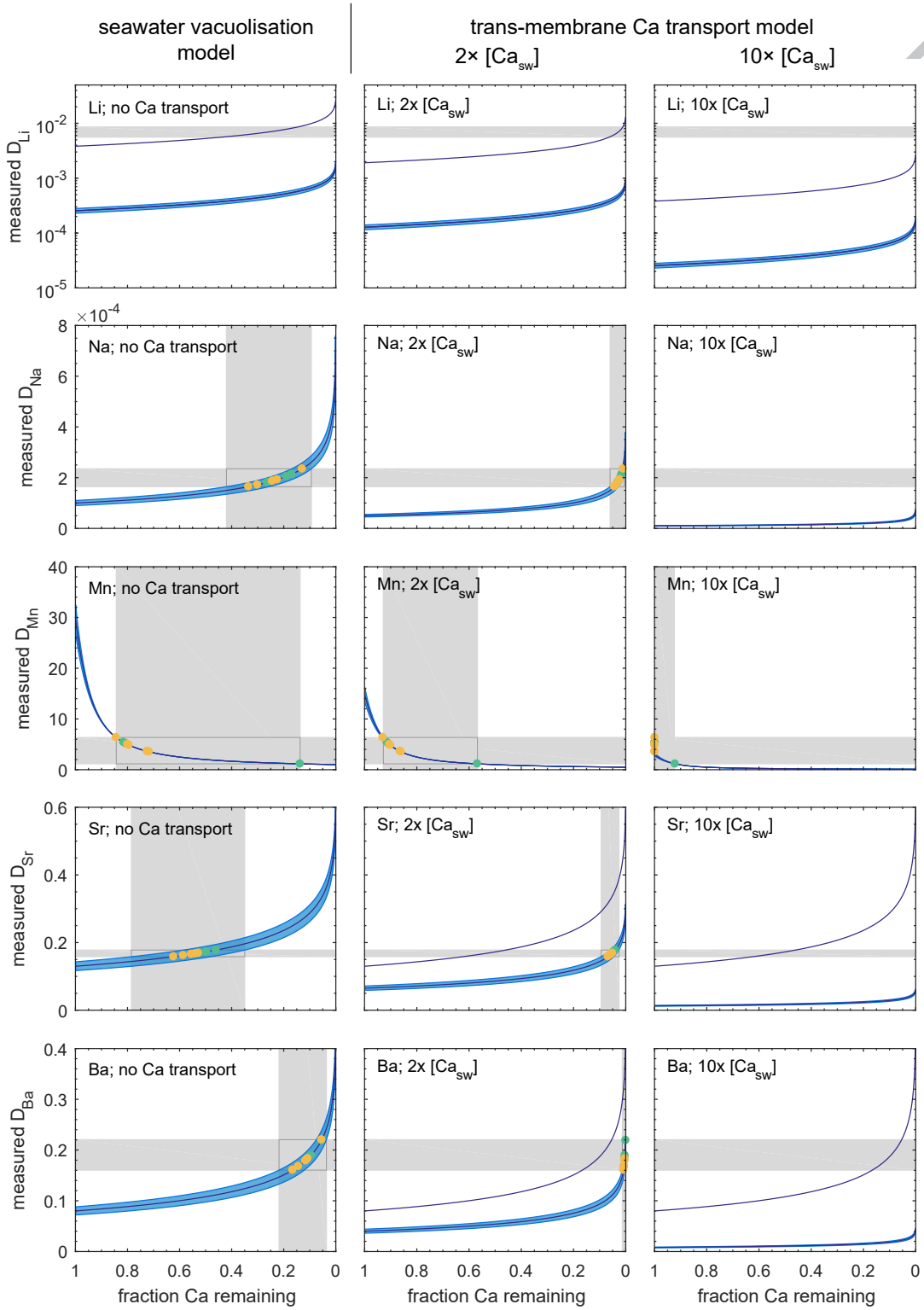

Figure 4: See following page for caption.

Figure 4: Rayleigh fractionation modelling of *G. ruber* apparent trace element distribution coefficients (D_X = [X/Ca_{shell}]/[X/Ca_{sw}]), assuming that calcification takes place in a closed space. Blue lines with uncertainty intervals show the predicted evolution of trace element distribution coefficients with the fraction calcium utilised, based on inorganic calcite data (see text for details), including 10% uncertainty envelopes. *G. ruber* measurements (Tab. 4) are overlain in yellow (variable seawater chemistry, constant temperature) and green (variable temperature, constant seawater chemistry). Horizontal grey bars show the range of measured apparent distribution coefficients, vertical grey bars show the predicted calcium utilisation based on these. The left column displays this exercise assuming no modification of the seawater from which calcification takes place (the seawater vacuolisation model). The central and right columns show the impact of Ca transport on these results, if the Ca concentration is doubled (centre) and increased by a factor of 10 (right). All calculations assume that the trace element concentration of the calcifying fluid is equivalent to seawater. In the case of Li two curves are shown because there is uncertainty over which inorganic calcite distribution coefficient is applicable to foraminifera, see text for details. In the case of Sr/Ca and Ba/Ca endmember curves are shown depicting both complete selectivity of Ca channels over Sr and Ba (model with 10% uncertainty envelopes), and complete non-selectivity, i.e. no preferential transport of Ca over Sr or Ba (thin purple line). Note the logarithmic D_{Li} scale, necessary in order to highlight that *G. ruber* Li concentrations are several orders of magnitude higher than expected in all models.

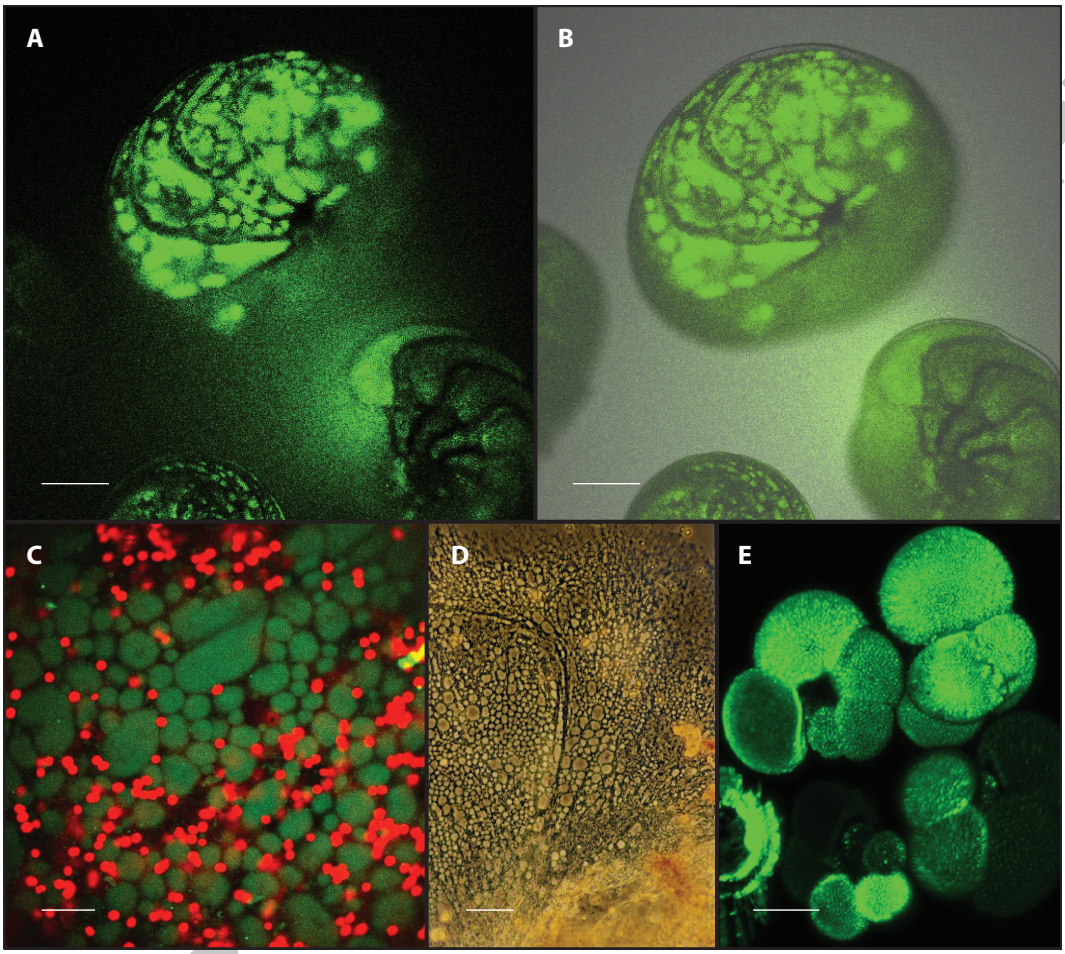

Figure 5: Seawater vacuolisation images in cultured *Amphistegina lessonii*. (A) Fluorescent image of foraminifera placed into seawater with 40 μM calcein for several hours, and then immediately transferred into calcein-free seawater. Individual large seawater vacuoles can be seen through the thin chamber walls, which take up most of the space in the last six chambers of the top individual. Note that the specimen on the right was not active during this experiment. Scale bar 100 μm. (B) As panel A, with the transparent (non fluorescent) channel overlain. (C) Close-up view of calcein-containing seawater vacuoles in a recovering individual (see Bentov and Erez, 2005). Scale bar 20 μm. The red fluorescent spots are diatom symbionts. (D) Transmitted light image of the site of chamber formation in a recovering individual showing the abundance of vacuoles. Scale bar 50 μm. (E) Calcein-labelled planktonic foraminifera, demonstrating that seawater is present at the calcification site in planktonic as well as benthic species. Scale bar 50 μm.

Table 1: Carbonate chemistry details of seawater reservoirs used in the *O. ammonoides* culture experiments. All experiments were conducted at 25°C and 37 psu. DIC and $\Omega_{calcite}$ were calculated using co2sys (Lewis and Wallace, 1998), using the same parameters as Raitzsch et al. (2010). Errors represent 1SD variation based on replicate measurements over the course of the experimental period.

Exp.	Alkalinity (mEq l^{-1})	pH (total scale)	DIC (μM)	$\Omega_{calcite}$
DE5: Variable DIC, constant pH				
DE5-1	2654±11	7.97±0.04	2357	5.27
DE5-2	2241±10	8.00±0.06	1961	4.65
DE5-3	1764±7	8.00±0.11	1525	3.61
DE5-4	2063±11	8.03±0.08	1779	4.55
DE5: Variable pH, constant DIC				
DE5-5	2403±10	8.23±0.06	1955	7.37
DE5-6	2270±11	8.10±0.04	1927	5.61
DE5-7	2142±10	7.78±0.05	1975	2.97
DE5-8	2020±7	7.46±0.06	1970	1.45

Table 2: Seawater elemental chemistry of all culture experiments. F_{ASW} denotes the proportion of the seawater reservoir that was derived from Mg-free artificial seawater. See text for notes on Mn data.

Exp.	F_{ASW}	$[Ca_{sw}]$ (mM)	Li/Ca (mmol/mol)	Na/Ca (mol/mol)	Mg/Ca (mol/mol)	Mn/Ca (μmol/mol)	Sr/Ca (mmol/mol)	Ba/Ca (μmol/mol)
DE5 (*O. ammonoides*): Variable DIC, constant pH								
DE5	0	10.9	2.03	45.7	5.16	0.4	8.62	4.7
DE3 (*G. ruber*): Variable Mg/Ca_{sw}								
DE3-2	0.6	12.1	0.84	46.5	2.14	0.4	8.30	16.3
DE3-3	0.4	11.8	1.36	47.0	3.21	0.4	8.65	12.5
DE3-4	0.2	11.4	1.57	45.7	4.10	0.4	8.39	8.2
DE3-5	0	11.4	2.31	45.6	5.13	0.4	8.88	4.5
DE3-6	0	10.7	1.95	45.2	6.17	0.4	8.56	5.1
DE5 (*G. ruber*): Variable temperature at low Mg/Ca_{sw}								
DE4	0.4	11.3	1.34	46.9	3.36	0.4	8.38	4.6

Table 3: Results of the *O. ammonoides* carbonate chemistry experiment. Mean growth rate is determined from alkalinity depletion of the culture seawater, measured and replaced every three to four days. The fraction of specimens that calcified is based on the proportion of foraminifera with at least one chamber with $^{135}Ba/^{138}Ba$ within error of the spiked culture seawater (see text for details), and represents a worst case end-member in terms of the number of calcifying specimens. Normalised growth rate = mean growth rate/fraction of specimens that calcified.

Exp.	pH (total)	DIC (μM)	Mean growth rate (μg ind.$^{-1}$ day^{-1})	Fraction calcifying	n	Normalised growth rate	Mg/Ca (mmol/mol)
DE5-1	8.00	2357	59.8	0.11	19	478.1	143.7±3.0
DE5-2	8.04	1961	85.6	0.40	5	195.6	146.5±3.0
DE5-3	8.07	1525	85.2	0.38	8	189.4	143.5±4.1
DE5-4	8.11	1779	11.9	0.09	16	118.5	144.0±4.5
DE5-5	8.30	1955	63.8	0.39	7	212.8	153.3±1.5
DE5-6	8.15	1927	61.8	0.09	23	329.5	150.1±2.7
DE5-7	7.84	1975	57.5	0.16	29	306.7	139.6±2.7
DE5-8	7.53	1970	38.3	0.20	7	153.3	143.4±2.1

Table 4: Laser-ablation ICPMS trace element data of *G. ruber* cultured under variable seawater Mg/Ca and temperature. See Tab. 2 for seawater Mg/Ca ratios, culture temperatures are given in brackets after the experiment names. Na/Ca, Mg/Ca and Sr/Ca ratios are given in mmol mol^{-1}. Li/Ca, Mn/Ca and Ba/Ca are given in μmol mol^{-1}. All errors are 2SE. Note that the stated D_{Mn} represent minimum values, see text for details.

Exp.	Li/Ca	D_{Li}	Na/Ca	D_{Na}	Mg/Ca	D_{Mg}	Mn/Ca	D_{Mn}	Sr/Ca	D_{Sr}	Ba/Ca	D_{Ba}
DE3-6 (26)	14.4±0.7	0.0068	7.77±0.20	0.17	6.80±0.21	0.0011	1.5±0.7	3.9	1.43±0.01	0.17	0.89±0.02	0.17
DE3-5 (26)	14.2±0.6	0.0056	10.72±0.67	0.24	6.37±1.19	0.0012	2.4±0.6	6.0	1.47±0.02	0.17	1.02±0.07	0.23
DE3-4 (26)	14.8±2.9	0.0086	8.79±1.03	0.19	5.38±1.48	0.0013	2.9±2.9	7.3	1.42±0.06	0.17	1.48±0.21	0.18
DE3-3 (26)	11.0±0.6	0.0075	8.77±0.23	0.19	4.38±0.25	0.0014	2.7±0.6	6.6	1.37±0.02	0.16	2.34±0.19	0.19
DE3-2 (26)	6.4 ±0.3	0.0070	7.65±0.22	0.16	3.03±0.14	0.0014	2.9±0.3	7.2	1.35±0.01	0.16	2.59±0.12	0.16
DE4-3 (27.5)	10.5±0.4	0.0070	8.61±0.26	0.18	3.84±0.39	0.0011	0.2±0.4	0.5	1.44±0.02	0.17	0.80±0.04	0.17
DE4-3 (25)	9.8±0.3	0.0070	9.91±0.20	0.21	3.12±0.19	0.0009	1.3±0.3	3.1	1.43±0.01	0.17	0.80±0.02	0.18
DE4-3 (22.5)	10.8±1.1	0.0077	8.73±0.39	0.19	2.53±0.08	0.0008	1.2±1.1	3.0	1.43±0.08	0.17	0.83±0.02	0.19
DE4-3 (20)	9.0±0.2	0.0064	9.50±0.32	0.21	2.23±0.15	0.0007	n.d.	n.d.	1.47±0.00	0.18	0.96±0.06	0.22

References

Allen, G. J., Sanders, D., 1994. Two voltage-gated, calcium release channels coreside in the vacuolar membrane of broad bean guard cells. The Plant Cell 6 (5), 685–694.

Allen, K. A., Hönisch, B., Eggins, S. M., Haynes, L. L., Rosenthal, Y., Yu, J., 2016. Trace element proxies for surface ocean conditions: A synthesis of culture calibrations with planktic foraminifera. Geochimica et Cosmochimica Acta 193, 197–221.

Aoki, I., Tanaka, C., Takegami, T., Ebisu, T., Umeda, M., Fukunaga, M., Fukuda, K., Silva, A. C., Koretsky, A. P., Naruse, S., 2002. Dynamic activity-induced manganese-dependent contrast magnetic resonance imaging (DAIM MRI). Magnetic resonance in medicine 48 (6), 927–933.

Bach, L. T., 2015. Reconsidering the role of carbonate ion concentration in calcification by marine organisms. Biogeosciences 12 (16), 4939–4951.

Bentov, S., Brownlee, C., Erez, J., 2009. The role of seawater endocytosis in the biomineralization process in calcareous foraminifera. Proceedings of the National Academy of Sciences 106 (51), 21500–21504.

Bentov, S., Erez, J., 2005. Novel observations on biomineralization processes in foraminifera and implications for Mg/Ca ratio in the shells. Geology 33 (11), 841–844.

Bentov, S., Erez, J., 2006. Impact of biomineralization processes on the Mg content of foraminiferal shells: A biological perspective. Geochemistry Geophysics Geosystems 7 (1), Q01P08.

911 Bernhard, J. M., Blanks, J. K., Hintz, C. J., Chandler, G. T., 2004. Use of
912 the fluorescent calcite marker calcein to label foraminiferal tests. Journal of
913 foraminiferal Research 34 (2), 96–101.

914 Blue, C., Giuffre, A., Mergelsberg, S., Han, N., De Yoreo, J., Dove, P., 2017.
915 Chemical and physical controls on the transformation of amorphous calcium
916 carbonate into crystalline $CaCO_3$ polymorphs. Geochimica et Cosmochimica
917 Acta 196, 179–196.

918 Bryan, S., Marchitto, T., 2008. Mg/Ca–temperature proxy in benthic foraminifera:
919 New calibrations from the Florida Straits and a hypothesis regarding Mg/Li.
920 Paleoceanography 23 (2), PA2220.

921 Burton, E., Walter, L., 1991. The effects of pCO_2 and temperature on magnesium
922 incorporation in calcite in seawater and $MgCl_2$-$CaCl_2$ solutions. Geochimica et
923 Cosmochimica Acta 55 (3), 777–785.

924 Chester, R., Stoner, J., 1974. The distribution of zinc, nickel, manganese, cad-
925 mium, copper, and iron in some surface waters from the world ocean. Marine
926 Chemistry 2 (1), 17–32.

927 Dawber, C., Tripati, A., 2012. Relationships between bottom water carbonate sat-
928 uration and element/Ca ratios in coretop samples of the benthic foraminifera
929 *Oridorsalis umbonatus*. Biogeosciences 9 (8), 3029–3045.

930 de Choudens-Sánchez, V., González, L. A., 2009. Calcite and aragonite precip-
931 itation under controlled instantaneous supersaturation: Elucidating the role of
932 $CaCO_3$ saturation state and Mg/Ca ratio on calcium carbonate polymorphism.
933 Journal of Sedimentary Research 79 (6), 363–376.

de Nooijer, L. J., Spero, H., Erez, J., Bijma, J., Reichart, G.-J., 2014. Biomineralization in perforate foraminifera. Earth-Science Reviews 135, 48–58.

de Nooijer, L. J., Toyofuku, T., Kitazato, H., 2009. Foraminifera promote calcification by elevating their intracellular pH. Proceedings of the National Academy of Sciences 106 (36), 15374–15378.

Delaney, M., Bé, A. W. H., Boyle, E. A., 1985. Li, Sr, Mg, and Na in foraminiferal calcite shells from laboratory culture, sediment traps, and sediment cores. Geochimica et Cosmochimica Acta 49 (6), 1327–1341.

Dissard, D., Nehrke, G., Reichart, G.-J., Bijma, J., 2010. Impact of seawater pCO_2 on calcification and Mg/Ca and Sr/Ca ratios in benthic foraminifera calcite: results from culturing experiments with *Ammonia tepida*. Biogeosciences 7, 81–93.

Dissard, D., Nehrke, G., Reichart, G. J., Nouet, J., Bijma, J., 2009. Effect of the fluorescent indicator calcein on mg and sr incorporation into foraminiferal calcite. Geochemistry, Geophysics, Geosystems 10 (11).

Eggins, S., De Deckker, P., Marshall, J., 2003. Mg/Ca variation in planktonic foraminifera tests: implications for reconstructing palaeo-seawater temperature and habitat migration. Earth and Planetary Science Letters 212 (3-4), 291–306.

Elderfield, H., Bertram, C., Erez, J., 1996. A biomineralization model for the incorporation of trace elements into foraminiferal calcium carbonate. Earth and Planetary Science Letters 142 (3-4), 409–423.

Elderfield, H., Ferretti, P., Greaves, M., Crowhurst, S., McCave, I., Hodell, D.,

Piotrowski, A., 2012. Evolution of ocean temperature and ice volume through the mid-Pleistocene climate transition. Science 337 (6095), 704–709.

Elderfield, H., Yu, J., Anand, P., Kiefer, T., Nyland, B., 2006. Calibrations for benthic foraminiferal Mg/Ca paleothermometry and the carbonate ion hypothesis. Earth and Planetary Science Letters 250 (3-4), 633–649.

Erez, J., 2003. The source of ions for biomineralization in foraminifera and their implications for paleoceanographic proxies. Reviews in mineralogy and geochemistry 54 (1), 115–149.

Evans, D., Bhatia, R., Stoll, H., Müller, W., 2015a. LA-ICPMS Ba/Ca analyses of planktic foraminifera from the Bay of Bengal: Implications for late Pleistocene orbital control on monsoon freshwater flux. Geochemistry, Geophysics, Geosystems 16 (8), 2598–2618.

Evans, D., Brierley, C., Raymo, M. E., Erez, J., Müller, W., 2016a. Planktic foraminifera shell chemistry response to seawater chemistry: Pliocene–Pleistocene seawater Mg/Ca, temperature and sea level change. Earth and Planetary Science Letters 438, 139–148.

Evans, D., Erez, J., Oron, S., Müller, W., 2015b. Mg/Ca-temperature and seawater-test chemistry relationships in the shallow-dwelling large benthic foraminifer *Operculina ammonoides*. Geochimica et Cosmochimica Acta 148, 325–342.

Evans, D., Müller, W., 2012. Deep time foraminifera Mg/Ca paleothermometry: Nonlinear correction for secular change in seawater Mg/Ca. Paleoceanography 27, PA4205.

Evans, D., Müller, W., 2018. Automated extraction of a 5-year LA-ICPMS trace element dataset of ten common glass and carbonate standards: Long-term data quality, optimisation and laser cell homogeneity. Geostandards and Geoanalytical Research.

Evans, D., Müller, W., Oron, S., Renema, W., 2013. Eocene seasonality and seawater alkaline earth reconstruction using shallow-dwelling large benthic foraminifera. Earth and Planetary Science Letters 381, 104–115.

Evans, D., Wade, B., Henehan, M., Erez, J., Müller, W., 2016b. Revisiting carbonate chemistry controls on planktic foraminifera Mg/Ca: implications for sea surface temperature and hydrology shifts over the Paleocene-Eocene Thermal Maximum and Eocene-Oligocene transition. Climate of the Past 12 (4), 819.

Fehrenbacher, J. S., Martin, P. A., 2014. Exploring the dissolution effect on the intrashell Mg/Ca variability of the planktic foraminifer *Globigerinoides ruber*. Paleoceanography 29.

Fehrenbacher, J. S., Russell, A. D., Davis, C. V., Gagnon, A. C., Spero, H. J., Cliff, J. B., Zhu, Z., Martin, P., 2017. Link between light-triggered Mg-banding and chamber formation in the planktic foraminifera *Neogloboquadrina dutertrei*. Nature Communications 8.

Felder, C. C., Singer-Lahat, D., Mathes, C., 1994. Voltage-independent calcium channels: Regulation by receptors and intracellular calcium stores. Biochemical pharmacology 48 (11), 1997–2004.

Fujita, K., Hikami, M., Suzuki, A., Kuroyanagi, A., Sakai, K., Kawahata, H.,

1001 Nojiri, Y., 2011. Effects of ocean acidification on calcification of symbiont-
1002 bearing reef foraminifers. Biogeosciences 8 (8), 2089–2098.

1003 Gray, W. R., Weldeab, S., Lea, D. W., Rosenthal, Y., Gruber, N., Donner, B.,
1004 Fischer, G., 2018. The effects of temperature, salinity, and the carbonate system
1005 on Mg/Ca in *Globigerinoides ruber* (white): A global sediment trap calibration.
1006 Earth and Planetary Science Letters 482, 607–620.

1007 Hall, J. M., Chan, L.-H., 2004. Li/Ca in multiple species of benthic and plank-
1008 tonic foraminifera: thermocline, latitudinal, and glacial-interglacial variation.
1009 Geochimica et Cosmochimica Acta 68 (3), 529–545.

1010 Hasiuk, F., Lohmann, K., 2010. Application of calcite Mg partitioning functions
1011 to the reconstruction of paleocean Mg/Ca. Geochimica et Cosmochimica Acta
1012 74 (23), 6751–6763.

1013 Henehan, M. J., Evans, D., Shankle, M., Burke, J. E., Foster, G. L., Anagnos-
1014 tou, E., Chalk, T. B., Stewart, J. A., Alt, C. H., Durrant, J., et al., 2017. Size-
1015 dependent response of foraminiferal calcification to seawater carbonate chem-
1016 istry. Biogeosciences 14 (13), 3287.

1017 Hönisch, B., Allen, K., Russell, A., Eggins, S., Bijma, J., Spero, H., Lea, D.,
1018 Yu, J., 2011. Planktic foraminifers as recorders of seawater Ba/Ca. Marine Mi-
1019 cropaleontology 79 (1), 52–57.

1020 Ishikawa, M., Ichikuni, M., 1984. Uptake of sodium and potassium by calcite.
1021 Chemical Geology 42 (1), 137–146.

1022 Jacob, D., Wirth, R., Agbaje, O., Branson, O., Eggins, S., 2017. Planktic foramin-
1023 ifera form their shells via metastable carbonate phases. Nature Communications
1024 8 (1), 1265.

1025 Jochum, K., Stoll, B., Herwig, K., Willbold, M., Hofmann, A., Amini, M., Aar-
1026 burg, S., Abouchami, W., Hellebrand, E., Mocek, B., et al., 2006. MPI-DING
1027 reference glasses for in situ microanalysis: New reference values for element
1028 concentrations and isotope ratios. Geochemistry Geophysics Geosystems 7 (2).

1029 Jochum, K., Weis, U., Stoll, B., Kuzmin, D., Yang, Q., Raczek, I., Jacob, D.,
1030 Stracke, A., Birbaum, K., Frick, D., et al., 2011. Determination of reference
1031 values for NIST SRM 610–617 glasses following ISO guidelines. Geostandards
1032 and Geoanalytical Research.

1033 Johnstone, H. J., Lee, W., Schulz, M., 2016. Effect of preservation state of plank-
1034 tonic foraminifera tests on the decrease in Mg/Ca due to reductive cleaning and
1035 on sample loss during cleaning. Chemical Geology 420, 23–36.

1036 Khalifa, G. M., Kirchenbuechler, D., Koifman, N., Kleinerman, O., Talmon, Y.,
1037 Elbaum, M., Addadi, L., Weiner, S., Erez, J., 2016. Biomineralization pathways
1038 in a foraminifer revealed using a novel correlative cryo-fluorescence–SEM–
1039 EDS technique. Journal of structural biology 196 (2), 155–163.

1040 Kisakürek, B., Eisenhauer, A., Bohm, F., Garbe-Schönberg, D., Erez, J., 2008.
1041 Controls on shell Mg/Ca and Sr/Ca in cultured planktonic foraminiferan, *Glo-*
1042 *bigerinoides ruber* (white). Earth and Planetary Science Letters 273 (3-4), 260–
1043 269.

Kitano, Y., Kanamori, N., Oomori, T., 1971. Measurements of distribution coefficients of strontium and barium between carbonate precipitate and solution – abnormally high values of distribution coefficients measured at early stages of carbonate solution formation. Geochemical Journal 4 (4), 183–206.

Langer, G., Nehrke, G., Thoms, S., Stoll, H., 2009. Barium partitioning in coccoliths of *Emiliania huxleyi*. Geochimica et Cosmochimica Acta 73 (10), 2899–2906.

Lea, D., Mashiotta, T., Spero, H., 1999. Controls on magnesium and strontium uptake in planktonic foraminifera determined by live culturing. Geochimica et Cosmochimica Acta 63 (16), 2369–2379.

Lea, D. W., Spero, H. J., 1994. Assessing the reliability of paleochemical tracers: Barium uptake in the shells of planktonic foraminifera. Paleoceanography 9 (3), 445–452.

Lear, C. H., Coxall, H. K., Foster, G. L., Lunt, D. J., Mawbey, E. M., Rosenthal, Y., Sosdian, S. M., Thomas, E., Wilson, P. A., 2015. Neogene ice volume and ocean temperatures: Insights from infaunal foraminiferal Mg/Ca paleothermometry. Paleoceanography 30 (11), 1437–1454.

Lear, C. H., Elderfield, H., Wilson, P. A., 2000. Cenozoic deep-sea temperatures and global ice volumes from Mg/Ca in benthic foraminiferal calcite. Science 287, 269–272.

Lewis, E., Wallace, D., 1998. Program developed for CO_2 system calculations. ORNL/CDIAC-105. Carbon Dioxide Information Analysis Center, Oak Ridge National Laboratory, US Department of Energy, Oak Ridge, Tennessee.

1067 Longerich, H., Jackson, S., Günther, D., 1996. Laser ablation inductively cou-
1068 pled plasma mass spectrometric transient signal data acquisition and analyte
1069 concentration calculation. Journal of Analytical Atomic Spectrometry 11 (9),
1070 899–904.

1071 Lorens, R. B., 1981. Sr, Cd, Mn and Co distribution coefficients in calcite as a
1072 function of calcite precipitation rate. Geochimica et Cosmochimica Acta 45 (4),
1073 553–561.

1074 Marriott, C. S., Henderson, G. M., Belshaw, N. S., Tudhope, A. W., 2004. Temper-
1075 ature dependence of δ^7li, δ^{44}ca and Li/Ca during growth of calcium carbonate.
1076 Earth and Planetary Science Letters 222 (2), 615–624.

1077 McCleskey, E., Almers, W., 1985. The Ca channel in skeletal muscle is a large
1078 pore. Proceedings of the National Academy of Sciences 82 (20), 7149–7153.

1079 Millero, F. J., 2013. Chemical oceanography, 4th Edition. CRC press.

1080 Mucci, A., 1988. Manganese uptake during calcite precipitation from seawater:
1081 conditions leading to the formation of a pseudokutnahorite. Geochimica et Cos-
1082 mochimica Acta 52 (7), 1859–1868.

1083 Mucci, A., Morse, J., 1983. The incorporation of Mg^{2+} and Sr^{2+} into calcite over-
1084 growths: influences of growth rate and solution composition. Geochimica et
1085 Cosmochimica Acta 47 (2), 217–233.

1086 Müller, M. N., Kısakürek, B., Buhl, D., Gutperlet, R., Kolevica, A., Riebesell,
1087 U., Stoll, H., Eisenhauer, A., 2011. Response of the coccolithophores *Emil-*
1088 *iania huxleyi* and *Coccolithus braarudii* to changing seawater Mg^{2+} and Ca^{2+}

concentrations: Mg/Ca, Sr/Ca ratios and $\delta^{44/40}$Ca, $\delta^{26/24}$Mg of coccolith calcite. Geochimica et cosmochimica acta 75 (8), 2088–2102.

Müller, W., Shelley, M., Miller, P., Broude, S., 2009. Initial performance metrics of a new custom–designed ArF excimer LA–ICPMS system coupled to a two-volume laser–ablation cell. Journal of Analytical Atomic Spectrometry 24 (2), 209–214.

Nehrke, G., Keul, N., Langer, G., de Nooijer, L., Bijma, J., Meibom, A., 2013. A new model for biomineralization and trace-element signatures of foraminifera tests 10, 9797–9818.

Nürnberg, D., Bijma, J., Hemleben, C., 1996. Assessing the reliability of magnesium in foraminiferal calcite as a proxy for water mass temperatures. Geochimica et Cosmochimica Acta 60 (5), 803–814.

Okumura, M., Kitano, Y., 1986. Coprecipitation of alkali metal ions with calcium carbonate. Geochimica et Cosmochimica Acta 50 (1), 49–58.

Oomori, T., Kaneshima, H., Maezato, Y., Kitano, Y., 1987. Distribution coefficient of Mg^{2+} ions between calcite and solution at 10–50°C. Marine Chemistry 20 (4), 327–336.

Pearce, N. J., Perkins, W. T., Westgate, J. A., Gorton, M. P., Jackson, S. E., Neal, C. R., Chenery, S. P., 1997. A compilation of new and published major and trace element data for NIST SRM 610 and NIST SRM 612 glass reference materials. Geostandards and Geoanalytical Research 21 (1), 115–144.

Raitzsch, M., Dueñas-Bohórquez, A., Reichart, G.-J., de Nooijer, L., Bickert, T., 2010. Incorporation of Mg and Sr in calcite of cultured benthic foraminifera:

impact of calcium concentration and associated calcite saturation state. Biogeosciences 7 (3), 869–881.

Raja, R., Saraswati, P., Rogers, K., Iwao, K., 2005. Magnesium and strontium compositions of recent symbiont-bearing benthic foraminifera. Marine Micropaleontology 58 (1), 31–44.

Reiss, Z., 1958. Classification of lamellar foraminifera. Micropaleontology 4 (1), 51–70.

Romani, A. M., Maguire, M. E., 2002. Hormonal regulation of Mg^{2+} transport and homeostasis in eukaryotic cells. Biometals 15 (3), 271–283.

Rosenthal, Y., Lear, C. H., Oppo, D. W., Linsley, B. K., 2006. Temperature and carbonate ion effects on Mg/Ca and Sr/Ca ratios in benthic foraminifera: Aragonitic species *Hoeglundina elegans*. Paleoceanography 21 (1).

Rosenthal, Y., Linsley, B. K., Oppo, D. W., 2013. Pacific ocean heat content during the past 10,000 years. Science 342 (6158), 617–621.

Rosenthal, Y., Morley, A., Barras, C., Katz, M. E., Jorissen, F., Reichart, G.-J., Oppo, D. W., Linsley, B. K., 2011. Temperature calibration of Mg/Ca ratios in the intermediate water benthic foraminifer *Hyalinea balthica*. Geochemistry, Geophysics, Geosystems 12 (4).

Russell, A., Hönisch, B., Spero, H., Lea, D., 2004. Effects of seawater carbonate ion concentration and temperature on shell U, Mg, and Sr in cultured planktonic foraminifera. Geochimica et cosmochimica acta 68 (21), 4347–4361.

1133 Sather, W. A., 2005. Voltage-gated calcium channels. Springer, Ch. 13, Selective
1134 permeability of voltage-gated calcium channels, pp. 205–218.

1135 Schiebel, R., 2002. Planktic foraminiferal sedimentation and the marine calcite
1136 budget. Global Biogeochemical Cycles 16 (4).

1137 Segev, E., Erez, J., 2006. Effect of Mg/Ca ratio in seawater on shell composition
1138 in shallow benthic foraminifera. Geochemistry, Geophysics, Geosystems 7 (2).

1139 Spero, H. J., Eggins, S. M., Russell, A. D., Vetter, L., Kilburn, M. R., Hönisch, B.,
1140 2015. Timing and mechanism for intratest Mg/Ca variability in a living planktic
1141 foraminifer. Earth and Planetary Science Letters 409, 32–42.

1142 Sviben, S., Gal, A., Hood, M. A., Bertinetti, L., Politi, Y., Bennet, M., Krish-
1143 namoorthy, P., Schertel, A., Wirth, R., Sorrentino, A., et al., 2016. A vacuole-
1144 like compartment concentrates a disordered calcium phase in a key coccol-
1145 ithophorid alga. Nature communications 7.

1146 ter Kuile, B., Erez, J., 1987. Uptake of inorganic carbon and internal carbon cy-
1147 cling in symbiont-bearing benthonic foraminifera. Marine Biology 94 (4), 499–
1148 509.

1149 ter Kuile, B., Erez, J., 1988. The size and function of the internal inorganic carbon
1150 pool of the foraminifer *Amphistegina lobifera*. Marine Biology 99 (4), 481–487.

1151 ter Kuile, B., Erez, J., Padan, E., 1989. Mechanisms for the uptake of inor-
1152 ganic carbon by two species of symbiont-bearing foraminifera. Marine Biology
1153 103 (2), 241–251.

1154 Titelboim, D., Sadekov, A., Almogi-Labin, A., Herut, B., Kucera, M., Schmidt,
1155 C., Hyams-Kaphzan, O., Abramovich, S., 2017. Geochemical signatures of
1156 benthic foraminiferal shells from a heat-polluted shallow marine environment
1157 provide field evidence for growth and calcification under extreme warmth run-
1158 ning. Global Change Biology 23 (10), 4346–4353.

1159 Toyofuku, T., Kitazato, H., Kawahata, H., Tsuchiya, M., Nohara, M., 2000. Eval-
1160 uation of Mg/Ca thermometry in foraminifera: Comparison of experimental
1161 results and measurements in nature. Paleoceanography 15, 456–464.

1162 Toyofuku, T., Matsuo, M. Y., De Nooijer, L. J., Nagai, Y., Kawada, S., Fujita, K.,
1163 Reichart, G.-J., Nomaki, H., Tsuchiya, M., Sakaguchi, H., et al., 2017. Proton
1164 pumping accompanies calcification in foraminifera. Nature Communications 8.

1165 van Dijk, I., de Nooijer, L. J., Reichart, G.-J., 2017. Trends in element incorpora-
1166 tion in hyaline and porcelaneous foraminifera as a function of pCO_2. Biogeo-
1167 sciences 14 (3), 497.

1168 Vigier, N., Rollion-Bard, C., Levenson, Y., Erez, J., 2015. Lithium isotopes in
1169 foraminifera shells as a novel proxy for the ocean dissolved inorganic carbon
1170 (DIC). Comptes Rendus Geoscience 347 (1), 43–51.

1171 Yu, J., Elderfield, H., 2008. Mg/Ca in the benthic foraminifera *Cibicidoides*
1172 *wuellerstorfi* and *Cibicidoides mundulus*: Temperature versus carbonate ion
1173 saturation. Earth and Planetary Science Letters 276 (1-2), 129–139.

1174 Zeebe, R. E., Bijma, J., Hönisch, B., Sanyal, A., Spero, H. J., Wolf-Gladrow,
1175 D. A., 2008. Vital effects and beyond: a modelling perspective on developing

palaeoceanographical proxy relationships in foraminifera. Geological Society, London, Special Publications 303 (1), 45–58.

Zeebe, R. E., Sanyal, A., 2002. Comparison of two potential strategies of planktonic foraminifera for house building: Mg^{2+} or h^{+} removal? Geochimica et Cosmochimica Acta 66 (7), 1159–1169.